1984

Microstructure and phase behavior of poly (para-phenylene benzobisthiazole)/methane sulfonic acid crystal solvates/

Herbert H. Frost
University of Massachusetts Amherst

MICROSTRUCTURE AND PHASE BEHAVIOR

OF

POLY (PARA-PHENYLENE BENZOBISTHIAZOLE)/METHANE SULFONIC ACID

CRYSTAL SOLVATES

A Thesis Presented

By

HERBERT HEMMING FROST

Submitted to the Graduate School of the
University of Massachusetts in partial fulfillment
of the requirements for the degree of

MASTER OF SCIENCE

September, 1984

Polymer Science and Engineering

MICROSTRUCTURE AND PHASE BEHAVIOR

OF

POLY (PARA-PHENYLENE BENZOBISTHIAZOLE)/METHANE SULFONIC ACID

CRYSTAL SOLVATES

A Thesis Presented

By

HERBERT HEMMING FROST

Approved as to style and content by:

Dr. Edwin L. Thomas,
Chairperson of Comittee

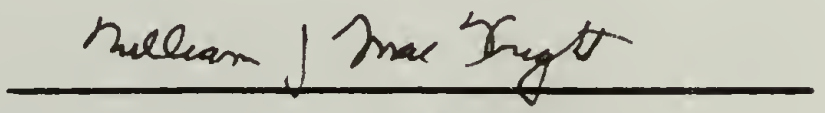

Dr. William J. MacKnight,
Department Head

ACKNOWLEDGEMENTS

I am grateful to the Air Force Materials Laboratory at Wright Patterson Air Force Base for the funding of this research.

Many thanks to Dr. Edwin L. Thomas for his friendship, advice and exhortation meted out in the proper doses at the proper times.

I am deeply grateful to Yachin Cohen for his counsel, fruitful discussions, both scientific and otherwise and especially his friendship.

My wife, Paula, was a tremendous help in innumerable ways. She typed the thesis in its various forms. She was my greatest fan and encourager. She provided a warm home environment to come to each evening. She prayed with faith and diligence for the successful completion of this thesis.

Finally, it is God who gives to men knowledge and understanding of all kinds of learning. I am forever thankful to Him for the modest success He has given. Mostly, I am thankful to Him for the knowledge of Himself he gives through Jesus Christ.

TABLE OF CONTENTS

LIST OF TABLES

LIST OF FIGURES

C H A P T E R 1

Introduction

The study of rigid rod macromolecules has received increasing attention in recent years due primarily to the fabrication of ultra-high modulus, ultra-high strength fibers and films from these materials. These polymers frequently exhibit unusually good thermo-oxidative stability and resistance to most common solvents.

Poly (p-phenylene benzobisthiazole) is a fully aromatic rigid rod polymer. Its properites have improved to a point of superiority among ultra-high strength ultra-high modulus fibers. Tension heat treatment as a last stage of processing has proven to be a most significant step in the attainment of the highest possible properties to date. Inveatigations of PBT have generally focused on two areas, either properties in solution or properties of the solid-state fiber or film. Only recently has the as-coagulated wet fiber been examined, and to date no thorough study linking the solid state and solutions through phase behavior has been performed. The solvent used in this study was methane sulfonic acid (MSA). The formation of the crystal solvate was induced by the diffusion of the atmospheric water into the system.

The purpose of this investigation is to characterize the structure and microstructure of quiescently crystal-

lized crystal solvates, to examine the crystalline polymer remaining upon removal of solvent from the solvate, and to relate these structures to the phase behavior of the PBT/MSA·H_2O system. Due to the excellent mechanical properites of PBT, crystal solvates should be of interest from a technological viewpoint to the extent that they affect the properties and processing of the final polymer product.

C H A P T E R II

Background

Polymer crystal solvates belong to the class of crystalline compounds whose lattice contains both solvent and solute in particular molar ratios. The most well known compounds of this type are the low molecular weight hydrates. That polymers form crystal solvates is not well known, although neither is it surprising. Bimolecular crystalline compounds arise from interactions such as hydrogen bonding or attractions between acidic and basic groups. That these interactions between a polymer and its solvent would give rise to a bimolecular crystalline formation is not unusual behavior. One of the reasons that little attention has been paid to these formations is that the majority of polymer processing takes place through the bulk melt phase, not through solution. For cellulose/sodium hydroxide system several crystal solvates of different stoichiometry have been observed, although they were simply described as swelling compounds [1]. With the advent of the aromatic polyamides, solution processing of another important class of polymers has become a significant industrial process. Not surprisingly, in recent years the number of instances where polymer crystal solvates have appeared in the literature has greatly increased, in conjunction with the increased interest in solution

processed polyamides. Iovleva and co-workers performed an extensive review of the literature in 1982 [2].

Evidence for the existence of polymer crystal solvates has been primarily by scattering and thermodynamic measurements. X-ray diffraction of polymer crystal solvates reveals unit cells which are expanded from those of the pure polymer. The thermodynamic measurements generally involve observation of a melting transition. Melting phenomena are experimentally observed in several ways. Polarizing optical microscopy shows the melting of birefringent crystal solvates into isotropic or anisotropic solutions. Differential scanning calorimetry also gives melting transition data, although it is often experimentally difficult to obtain due to the corrosive nature of the solvents. Finally, turbidity measurements have been used to determine the melting point of the PPTA/H_2SO_4 crystal solvates [3].

Poly(p-phenylene benzobisthiazole) is a fully aromatic rigid rod polymer. Its persistence length in chlorosulfonic acid has been determined to be 640 angstroms [4]. The PBT fibers investigated possess a high degree of axial orientation. Near perfect molecular alignment in the fiber direction has been shown by wide angle x-ray and electron diffraction studies. However true three dimensional order has not yet been achieved in any PBT fiber examined. Early diffraction studies done on as-spun PBT fibers were

explained by a hexagonal packing of axially staggered periodic cylinders. Upon heat treatment, the molecular order in the PBT fiber is enhanced and a two-dimensional net allowing the molecules translational freedom along the chain axis explains the diffraction data [18]. It has yet to be shown whether or not true large-scale three dimensional order is possible for PBT. Minter has shown the crystallite size in tension heat-treated PBT fibers to be 100 angstroms by 150 angstroms (lateral and longitudinal dimensions, respectively). Previous investigation of PBT coagulated from solution in the absence of shear has been limited. However for poly(p-phenylene benzobisoxazole), (PBO), another fully aromatic rigid rod polymer, Minter observed a fibrillar "grassy mat" in films prepared in this way [5]. He did not however investigate them any further to determine molecular orientation within the fibrils.

Takahashi has done the most extensive work on PPTA crystal solvates using both sulfuric acid and hexamethyl phosphorous triamide (HMPTA) as solvents. He found that at concentrations higher than 11% at room temperature, the PPTA/H_2SO_4 system formed a solid anisotropic phase. Optically negative spherulites were observed. Upon removal of solvent and observation under an electron microscope he observed 600 angstrom lamellae. The chain axis of the polymer was found to be perpendicular to the long axis of the lamellae [6]. Takahashi does not confirm the crystal

solvate nature of his solid anisotropic state; however, Platonov [7] and Iovleva [8] have independently confirmed the crystal solvate nature of the PPTA/H_2SO_4 anisotropic solid by x-ray diffraction.

The phase behavior giving rise to polymer crystal solvates is an outgrowth of theoretical phase behavior of rigid rod solutions. Onsager [9] and Isihara [10] independently predicted the possibility of liquid-liquid phase separation of solutions of anisotropic molecules. Their treatment was improved upon and simplified by Flory. He used a lattice model to predict the phase behavior [11]. His results have since been experimentally verified by others.

Ciferri and Krigbaum extended this phase behavior to include the crystallization of the polymer. By overlaying curves for crystallization from an isotropic solution and crystallization from an anisotropic solution, onto the Flory phase diagram, they obtained the phase diagram shown in Figure 2.1 [12]. Others have since made the step of inclusion of crystal solvates giving a schematic phase diagram as shown in Figure 2.2 [2]. A partial phase diagram including crystal solvates has been obtained by Gardner et al. [13] for the PPTA/H_2SO_4 system.

Miller has shown that treating a solvent and non-solvent as a single component is an appropriate assumption in the biphasic chimney region [14]. However, it is not

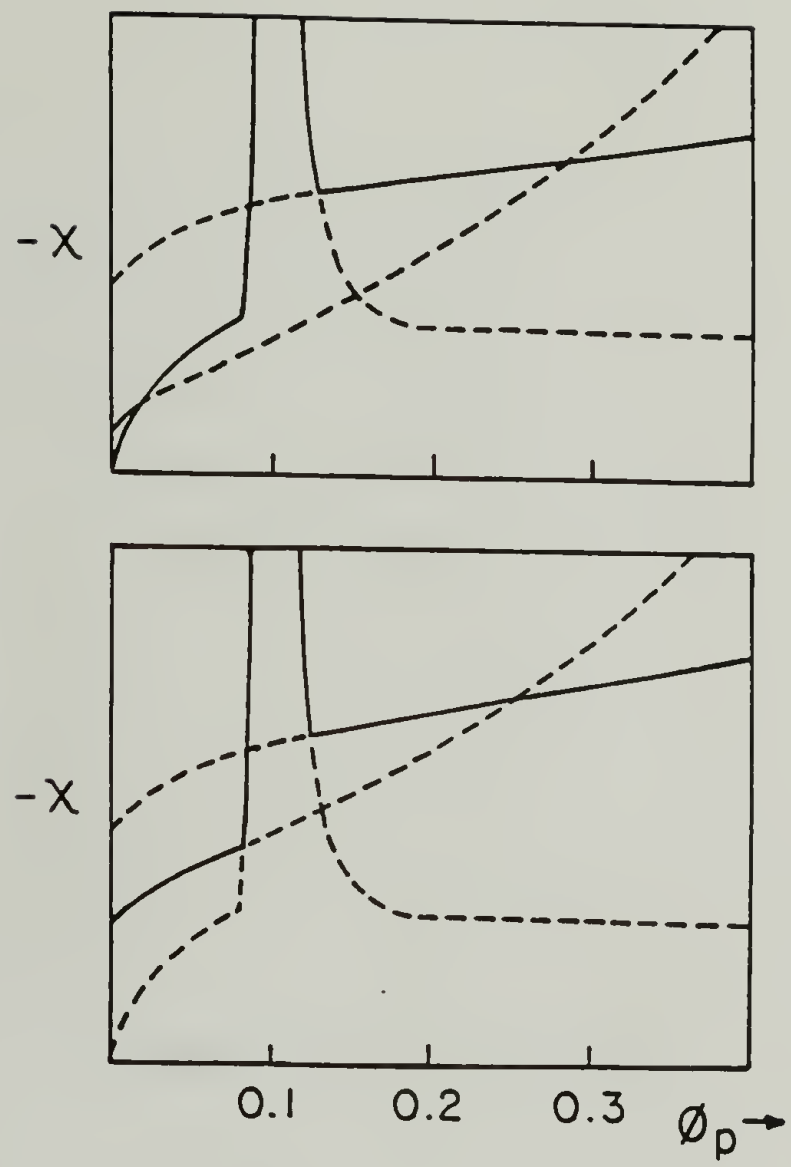

Figure 2.1

Superposition of liquid- liquid and solid-liquid phase diagrams. Top diagram is for a crystal having smaller melting transition temperature and heat of fusion; bottom diagram is for larger values.

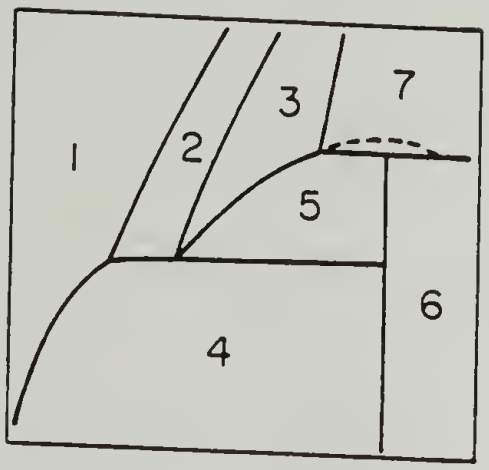

Figure 2.2

Schematic phase diagram for rigid-rod polymer with the inclusion of a crystal solvate.

1. isotropic solution
2. isotropic solution plus anisotropic solution
3. anisotropic solution
4. isotropic solution plus crystal solvate
5. anisotropic solution plus crystal solvate
6. crystal solvate plus crystalline polymer
7. crystalline polymer plus anisotropic solution

clear whether this assumption is viable in other regions. The reason for making this assumption is to aid in the kinetics of crystal growth. If one is in the isotropic solution region of the phase diagram at room temperature, a phase boundary can be crossed either by increasing the polymer concentration or by decreasing the temperature. Either course of action severely impedes chain mobility. Alternatively one can label the ordinate as $-\chi$ and cross the phase boundary by increasing the parameter by slight absorption of non-solvent, in this case water. Miller has shown that even a slight addition of non-solvent has a drastic effect on the location of the phase boundary [14]. Because of the ease of working with a binary phase diagram, and because of the improved kinetics when working at low concentrations at room temperature and above, this assumption and approach were made.

C H A P T E R III

EXPERIMENTAL

Materials

The PBT used was prepared by J.Wolfe of SRI via a step growth polymerization of 2.5 diamino-1, 4 benzenedithiol hydrochloride and phthalic acid conducted in poly (phosphoric acid). The polymer possessed an intrinsic viscosity of 2.0 in MSA. Crosby et al. calculated the molecular weight (M_η) of this polymer to be about 10,000 [4]. Since the monomer repeat molecular weight is 266 this corresponds to a molecular length of about 470 angstroms.

The solvent used was methane sulfonic acid from Aldrich Chemical Company.

Sample Preparation

The methane sulfonic acid as received contains about 1.5% water. This was purified using a vacuum distillation apparatus. Increments of PBT powder were added into the acid at room temperature, the polymer being used as received. Each incremental amount of PBT was dissolved before the next was added. For the purposes of this study samples of two to three milliliters of isotropic solution were prepared, generally to a concentration of two to five

percent polymer. These solutions were the starting point for all samples studied.

A cleaning solution for the glassware was made. Seventy grams of sodium dichromate were dissolved in 300 milliliters of water. Six hundred milliliters of sulfuric acid was then added. Glass slides and cover slips were placed into a beaker of this solution for about one hour at 60 degrees Celsius. Upon removal they were rinsed in copious amounts of water the final rinsings being done with deionized water.

A drop of solution was then placed on the clean dry slide and a clean dry cover slip was placed over the drop. Water diffusing in from the atmosphere induced the growth of the crystal solvate spherulites (e.g. Fig.3.1). After two to three days, sufficient water had diffused in to complete the phase separation into crystal solvate and dilute isotropic solution. The crystal solvate was then scraped from the slide into a DSC pan, or alternatively was placed onto a hot stage of an optical microscope.

For x-ray work the PBT/MSA solution was put into an x-ray capillary and the top was left open to air. As water diffused in the crystal solvate spherulites were induced to grow in the capillary. After several days the crystal solvate was grown and the capillary was sealed and x-ray diffraction was performed.

For electron microscopy the crystal solvates were

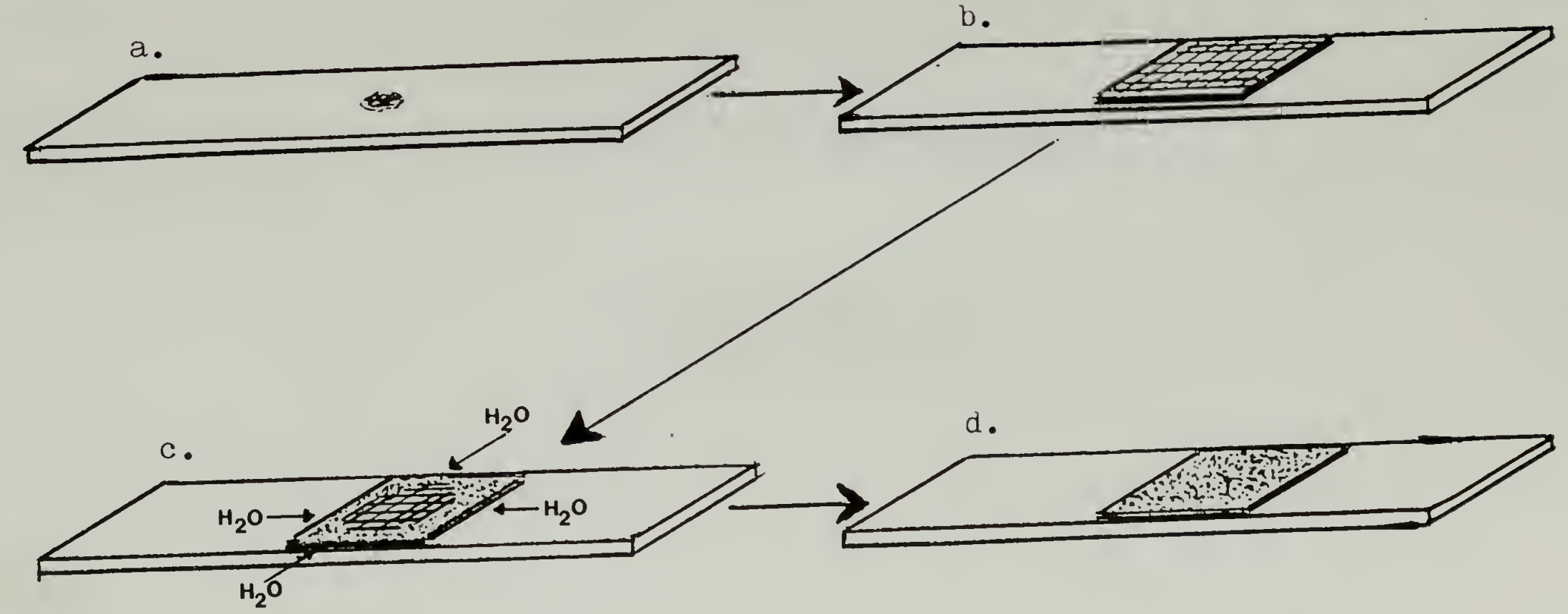

KEY:

 - Isotropic solution

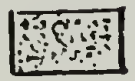 - Crystal solvate in equilibrium with dilute isotropic solution

Figure 3.1

a. drop of PBT/MSA solution is put on a clean glass slide, b. cover slip is placed over drop, c. water diffusing into the solution induces growth of crystal solvate, d. crystal solvate is fully grown.

melted (in the 90 to 100 degrees C range) and the now isotropic solution held at about 150 degrees C. As solvent was driven off, the solution went biphasic and new crystal solvate spherulites were observed to nucleate and grow. Once the crystal solvate was grown (a crystal solvate of different stoichiometry than that which melted at 90 degrees C) the cover slip and glass slide were split apart and the crystal solvate floated off onto water (e.g.Fig.3.2). This material was allowed to stand for several minutes and then picked up with gold microscope grids in order to avoid reaction of residual acid with copper grids. The sample was dried at room temperature and observed in the electron microscope. It was characteristic of these polymer spherulites that they had such high birefringerce that a sample thin enough to be used for electron microscopy was easily observable in the polarized optical microscope.

Electron Microscopy

A JEOL 100 CX electron microscope operated at 100 KV was used. Both bright field and dark field microscopy were performed in the conventional transmission mode. The diffraction data was generally collected using selected area diffraction. Preliminary studies of crystal solvate crystals were performed using micro-diffraction in the STEM mode. The radiation lifetime of PBT, following an

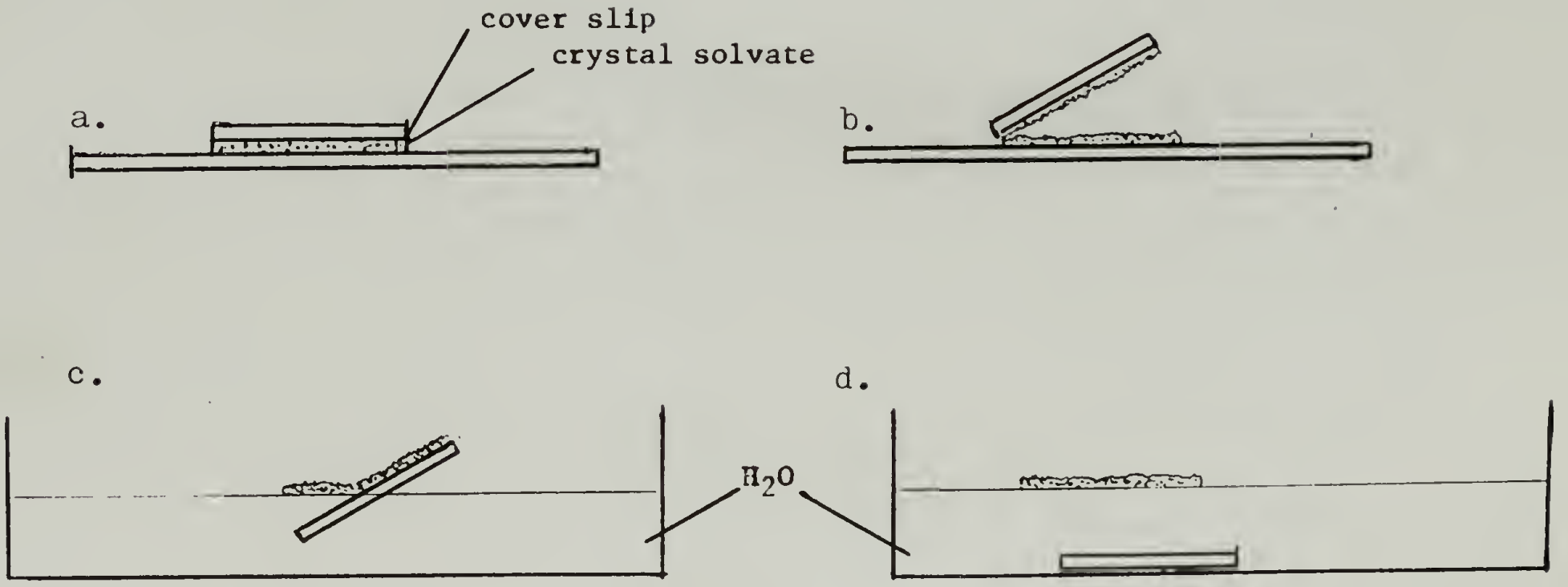

Figure 3.2

a. cover slip, crystal solvates, and glass slide, after heating at about 150°C, b. cover slip is split off, c. crystal solvate floated off onto deionized water, d. crystal solvate ready to be picked up with electron microscope grids.

exponential decay to 1/e of original intensity of crystalline reflections, was determined by Minter to be 1.6 coulombs per square centimeter or about two orders of magnitude greater than that of polyethylene. This stability allowed considerable latitude in selection of microscope imaging conditions.

An ETEC scanning electron microscope was used at 40 KV for the SEM studies of samples sputter coated with gold.

Optical Microscopy

A Zeiss polarizing microscope was used in conjunction with a Mettler FP-2 hot stage; and a Leitz polarizing microscope was used with a Leitz hot stage. Heating was generally done at a rate of 5 degrees C per minute. A quartz quarter waveplate was used to determine the sign of birefringence of the spherulites, direct comparison being made to optically negative poly(ethylene oxide) (PEO) spherulites.

X-Ray

Wide angle x-ray diffraction was performed with a flat-film Statton camera using CuK_α x-rays. Samples were flame sealed. Settings were 30 KV and 40 mA for exposure times of 4 to 10 hours. Sample to film distance was 53.14 mm.

DSC

A Perkin-Elmer DSC-2 was used for the calorimetry experiments, with indium and tin used for calibration purposes. The heating rate used was 10 degrees C per minute and a range of 10 mcal. Reusable gold plated stainless steel sample pans for volatile corrosives were used to prevent the MSA from corroding either the pan or the calorimeter.

C H A P T E R IV

RESULTS AND DISCUSSION

Results

The identification of the solid formed upon diffusion of water into the polymer/acid solution as crystal solvate involved two forms of evidence: melting transition(s) and expanded unit cell.

Figure 4.1 shows the DSC trace for the PBT/MSA·H_2O crystal solvate. In the corresponding temperature region the pure polymer has no thermal transitions. On the optical microscope there were three melting transitions observed. The first at 90 to 100 degrees C, the second at 135 to 200 degrees C and the third varied from 200 to 300 degrees C. Table 4.1 shows the relationship between the melting temperature observed optically and by DSC. The first two

Table 4.1
Melting behavior of PBT/MSA·H_2O crystal solvates

	T1	T2	T3
Opt. Micr.	90-100	135-200	varied:200-300
DSC	90-100	140-195	220-245

(All temperatures in degrees Celsius)

melting transitions correlate well. The discrepancy in the third melting temperature can be explained by the difference in the system for DSC and optical microscopy. For DSC the

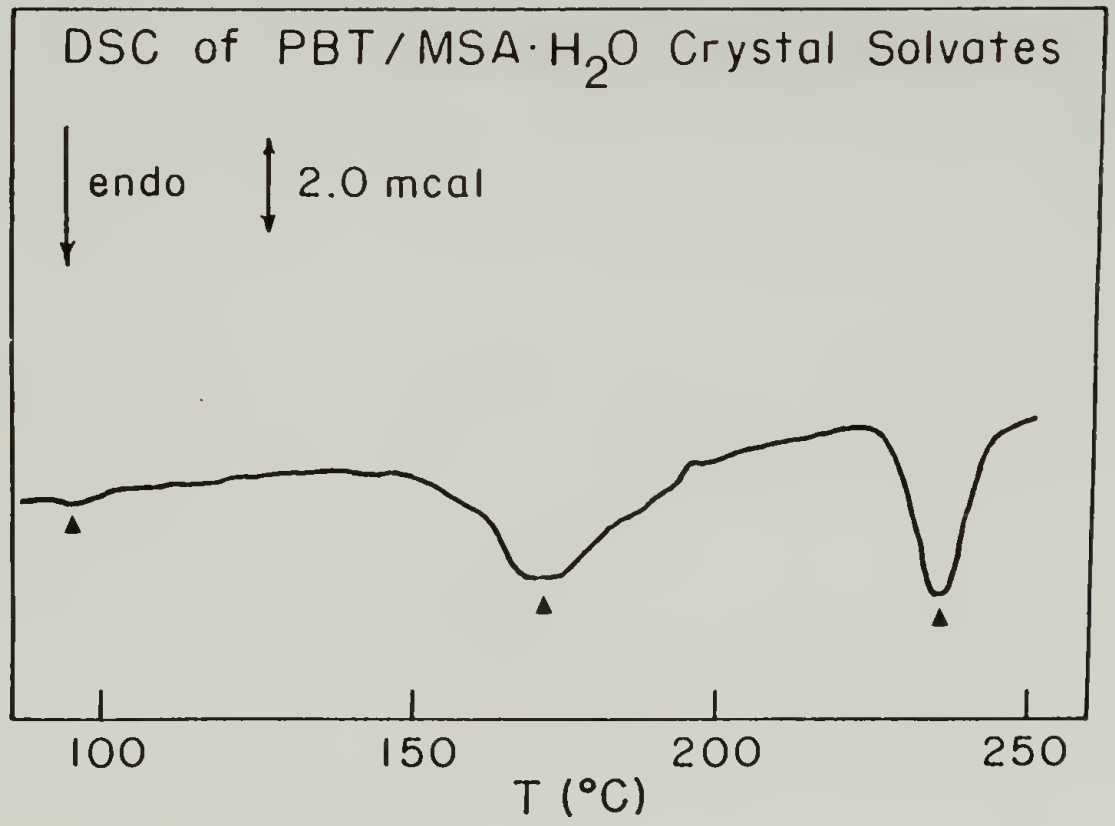

Figure 4.1

Differential scanning calorimeter trace of PBT/MSA·H_2O crystal solvates.

system is closed. The sample pans are sealed, allowing no escape of fumes. For optical microscopy, the sample was open to the atmosphere at the edge of the cover slip. White vapors were observed to escape at temperatures approaching 180 degrees C and above. Since the system consists of solvent and polymer, increasing the concentration of polymer by removal of solvent would tend to increase the equilibrium melting transition of the system. The time dependence of the melting transition at elevated temperature is supported by the fact that at very fast heating rates (ca. 30 degrees C per minute) the melting range is observed to be 200 degrees C to 220 degrees C. At very slow heating rates (ca. 2 degrees C per minute) the melting temperature was in the region of 295 to 305 degrees C. The slower the heating rate, the longer the time available for solvent to be driven off. This same effect is consistent with the slightly expanded range of the first melting transition.

The diffraction data in Table 4.2 shows the expanded unit cell characteristic of crystal solvates. Figure 4.2 is the flat film Statton photograph of the crystal solvate.

The spherulitic nature of these crystal solvates is clearly shown in the optical micrographs in Fig.4.3. The typical Maltese cross extinction pattern is shown under crossed polars. Washing and drying the spherulites followed by observation under a scanning electron microscope clearly confirms the spherulitic nature of the solid (e.g.Fig. 4.4).

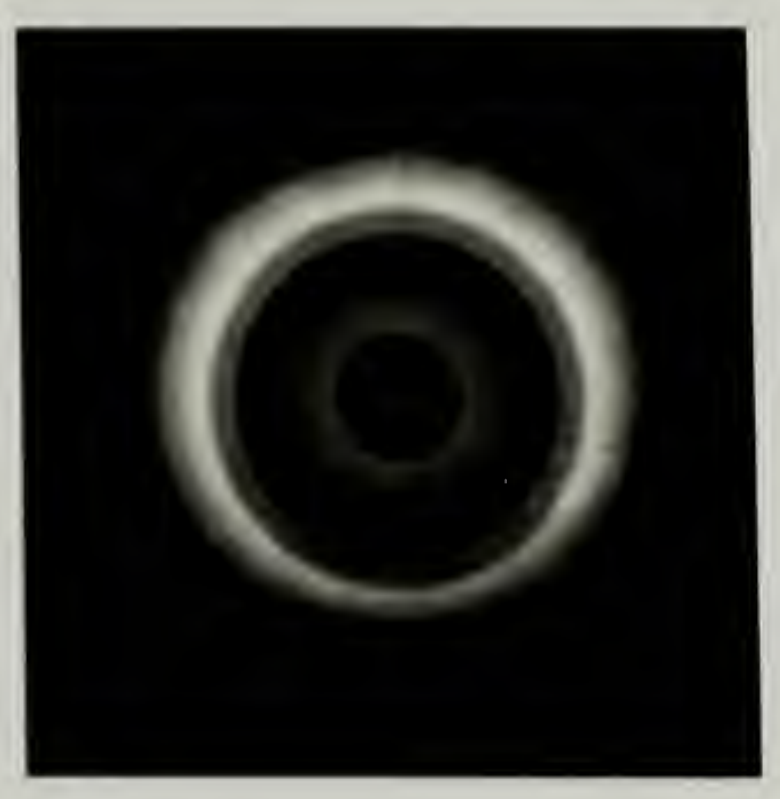

a.

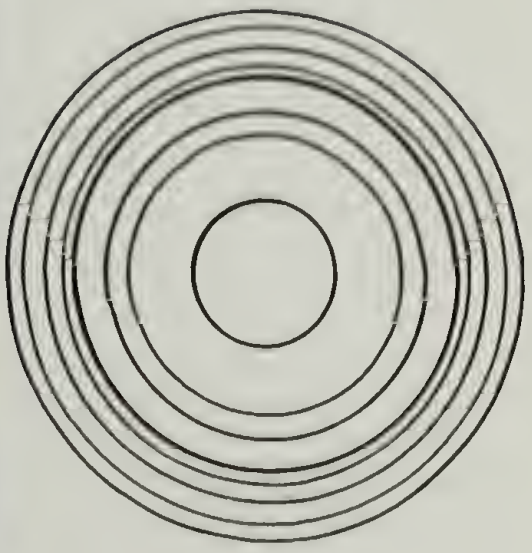

b.

Figure 4.2

a. Statton flat film x-ray diffraction of PBT/MSA·H_2O,
b. schematic of x-ray pattern.

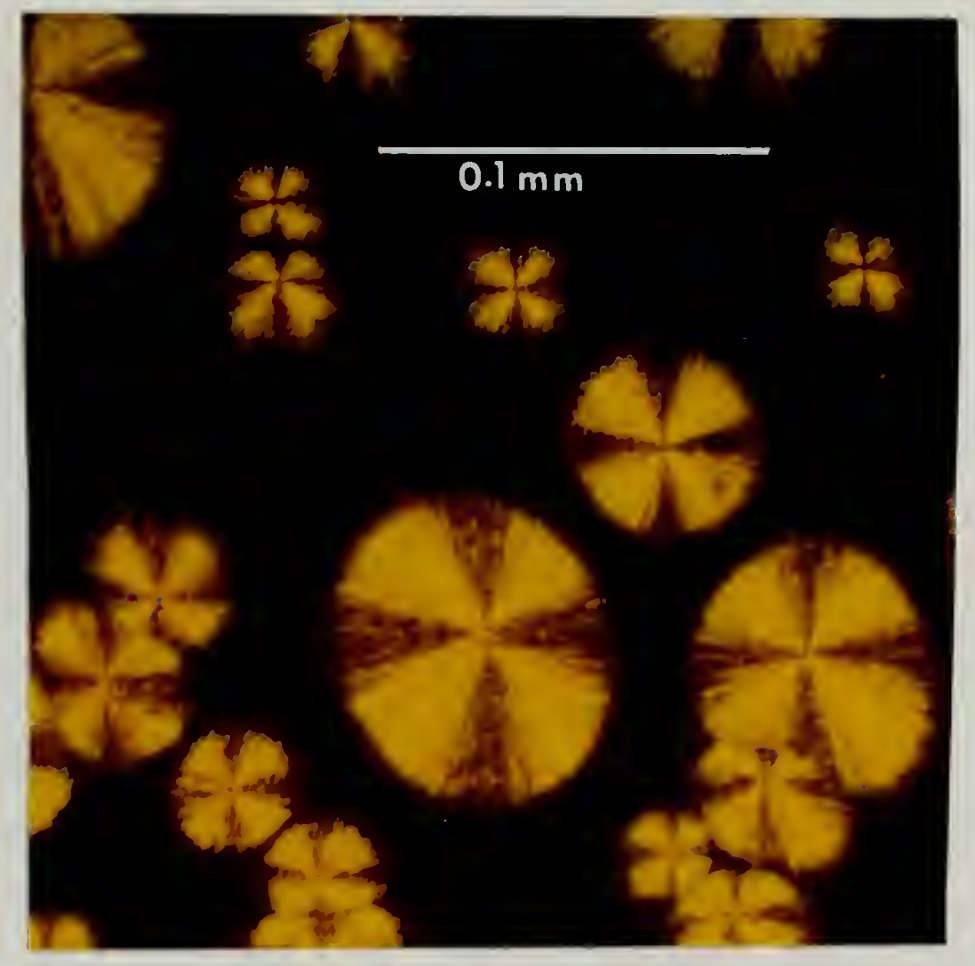

Figure 4.3

Typical Maltese cross extinction pattern of PBT/MSA·H_2O crystal solvate spherulites viewed under crossed polars in an optical microscope.

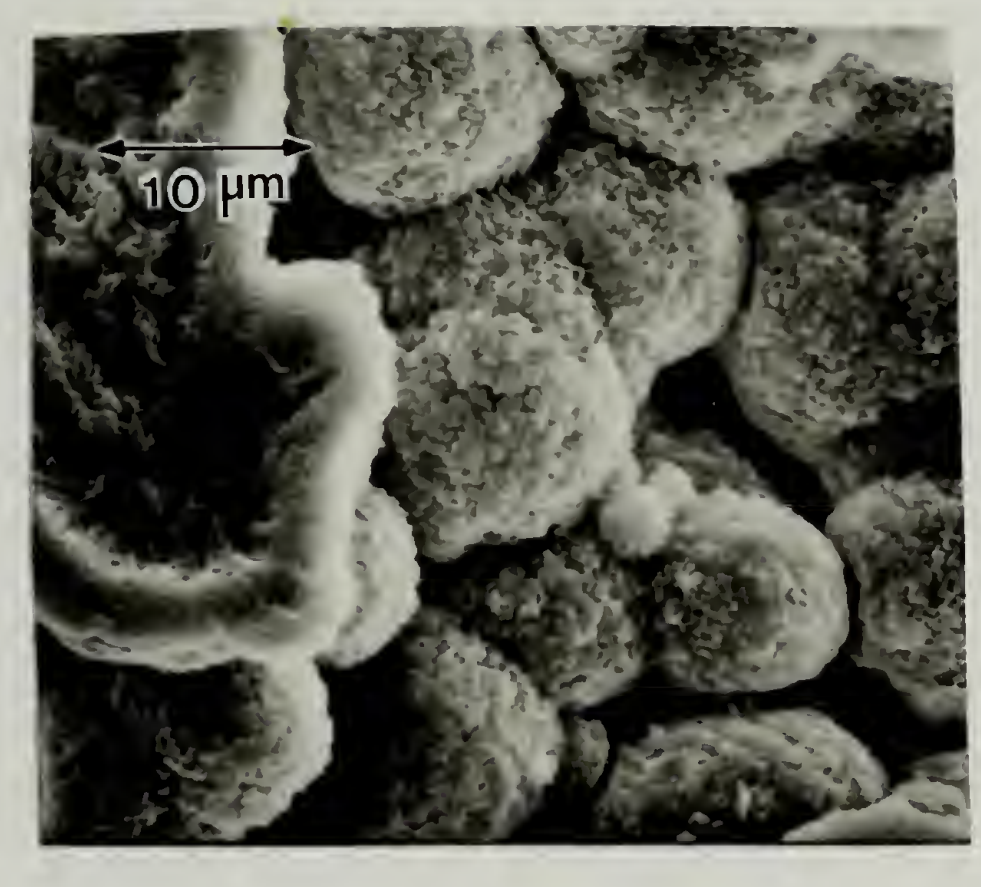

Figure 4.4

Scanning electron microscope photograph of PBT/MSA·H_2O spherulites having been washed in copious amounts of acetone and dried.

Table 4.2
Comparative diffraction of PBT fiber and crystal solvate

PBT fiber	PBT crystal solvate
12.45 m	12.45
5.9 e	7.45
3.54 e	5.2
3.18 e	4.5
2.94 e	4.2
	3.9
	3.6
	3.3
	2.6

m = meridional
e = equatorial
(All values of d spacings in angstroms)

Study of the PBT/MSA·H_2O crystal solvates confirmed several aspects of the schematic phase diagram given previously in Figure 2.2. Melting behavior of the crystal solvates was followed by optical microscopy. Figure 4.5 shows a sequence of photographs taken with increasing temperature. Each isolated area can be treated as a micro system. This has the disadvantage of not knowing the precise composition of each region, but, assuming heat transport is greater than mass transport, it allows the effect of temperature on a pseudo-equilibrium state to be followed simultaneously in several different regions. The first area to melt, as expected, is the area in communication with the droplet of solvent, and it is observed to melt into an isotropic solution. This corresponds to heating along path 'a' in Figure 4.6b. (Figure 4.6 represents a partial phase diagram showing the low polymer concentration region). Then

Figure 4.5

Optical micrographs showing melting of crystal solvates. a. at 27°C, b. at 92°C, c. at 94°C, d. and e. at 117°C. Note isotropic (1), anisotropic (2) and biphasic (3) liquid domains at 117°C equilibrium.

a. b. c.

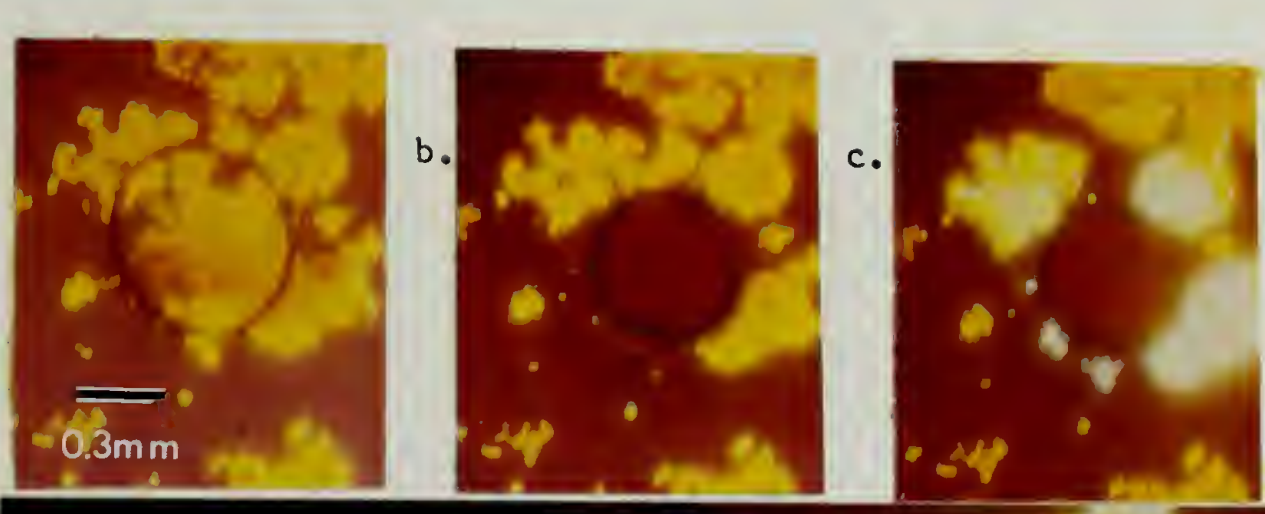

d.

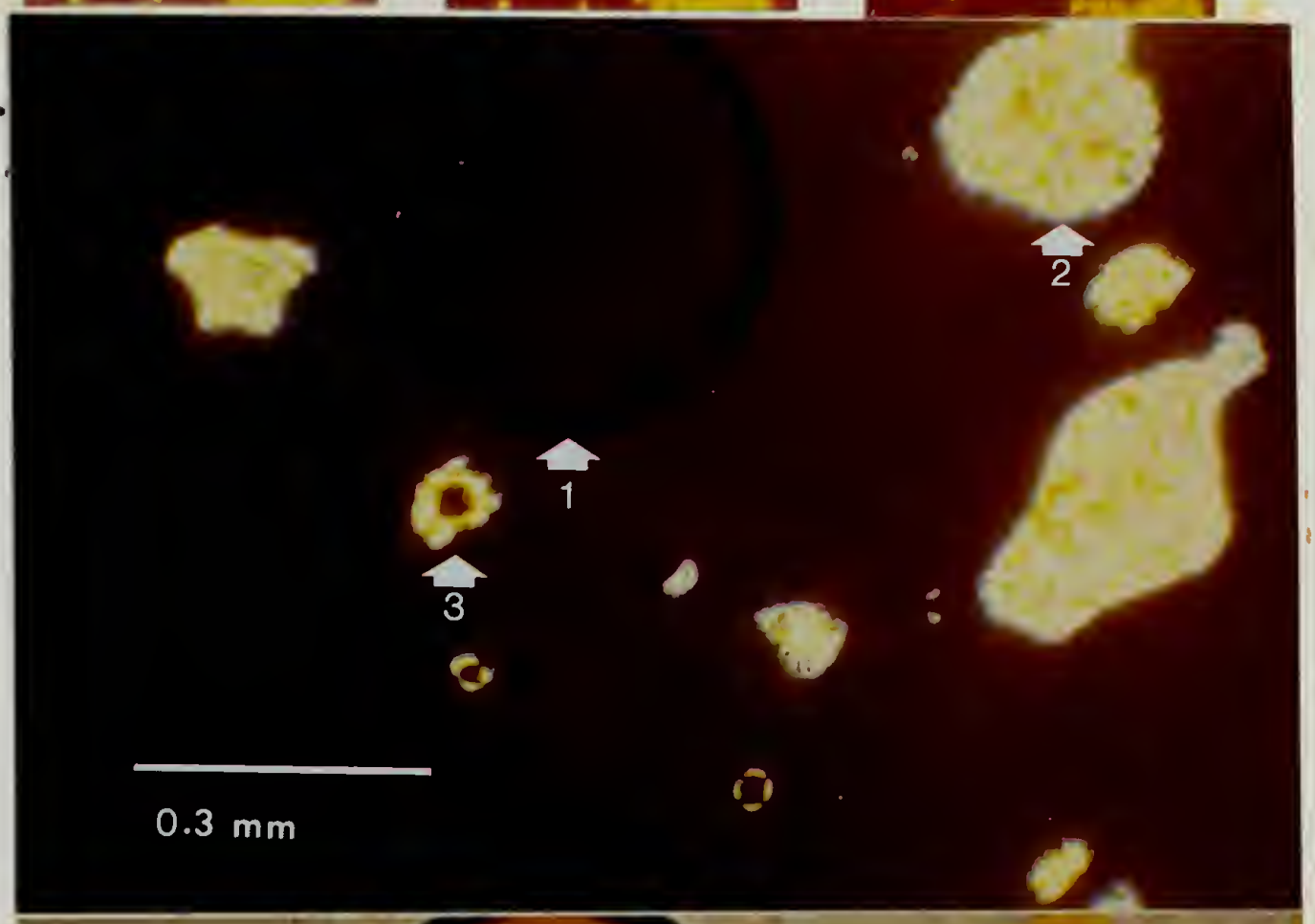

e.

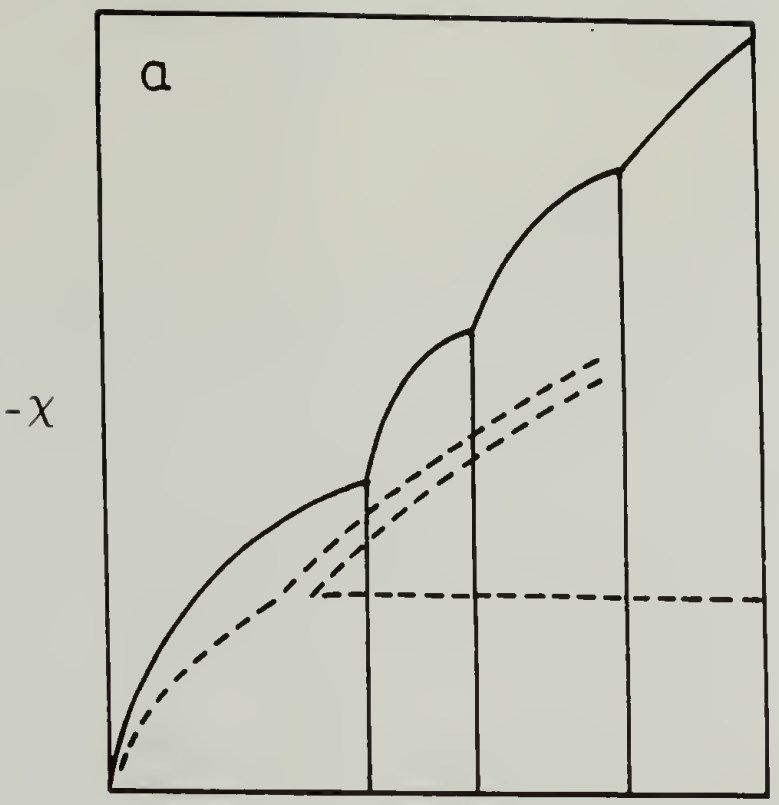

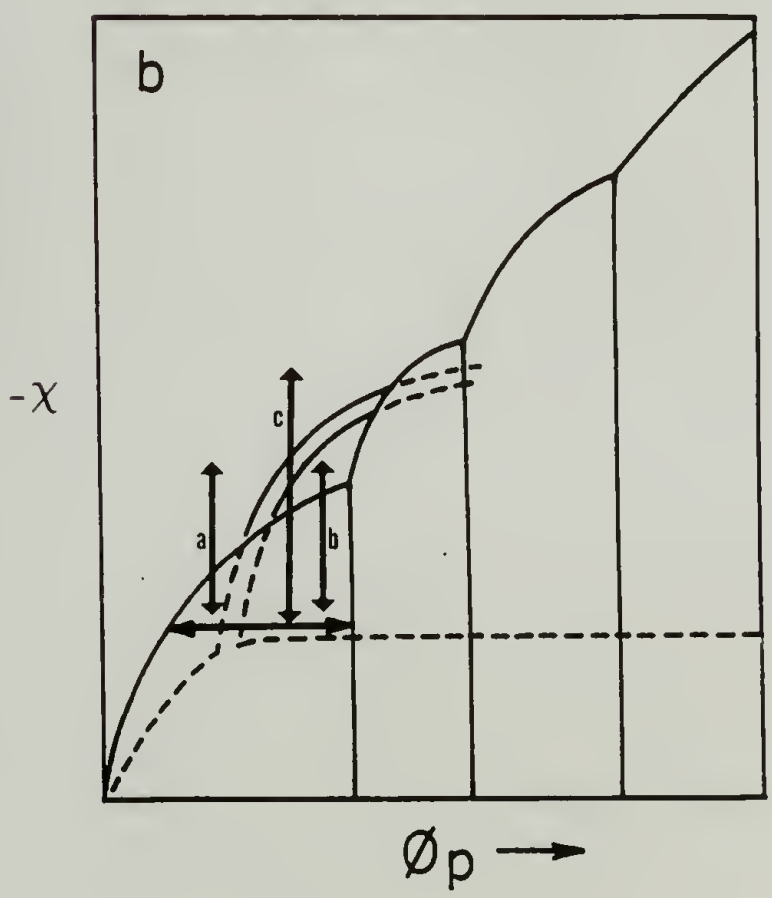

Figure 4.6

a. superposition of liquid-liquid and solid-liquid phase diagrams with the chimnev region inaccessible at equilibrium, b. with chimney region partially accessible at equilibrium.

the surrounding area which is not in communication with the isotropic drop melts into an anisotropic solution. This corresponds to heating along path 'b' in Figure 4.6b. Finally at steady state temperature of 117 degrees C three different types of micro systems are observed: isotropic, anisotropic and biphasic. This shows that the chimney region of the phase diagram is indeed above the crystallization boundary and not below it (e.g.Fig. 4.6a). This helps to explain the following observations: if the crystal solvates are melted into an isotropic solution (path 'c' of Figure 4.6b) and then cooled, the chimney region into the anisotropic region is crossed, for example, path 'c' of Figure 4.6b. With cooling to room temperature the anisotropic solution is metastable with respect to crystal solvates, and phase separation along the tie line shown to crystal solvate plus isotropic solution ensues (e.g.Fig. 4.7). The growth of the spherulite follows the typical stages of maturity and a brush type hedrite structure is shown in Figure 4.8.

Elucidation of the microstructure of the crystal solvate spherulites was complicated by the corrosive nature of the methane sulfonic acid. Utilization of a quartz quarter wave plate in a polarized optical microscope, and comparison with PEO optically negative spherulites showed that the PBT crystal solvate spherulites were optically negative. This means that the tangential index of

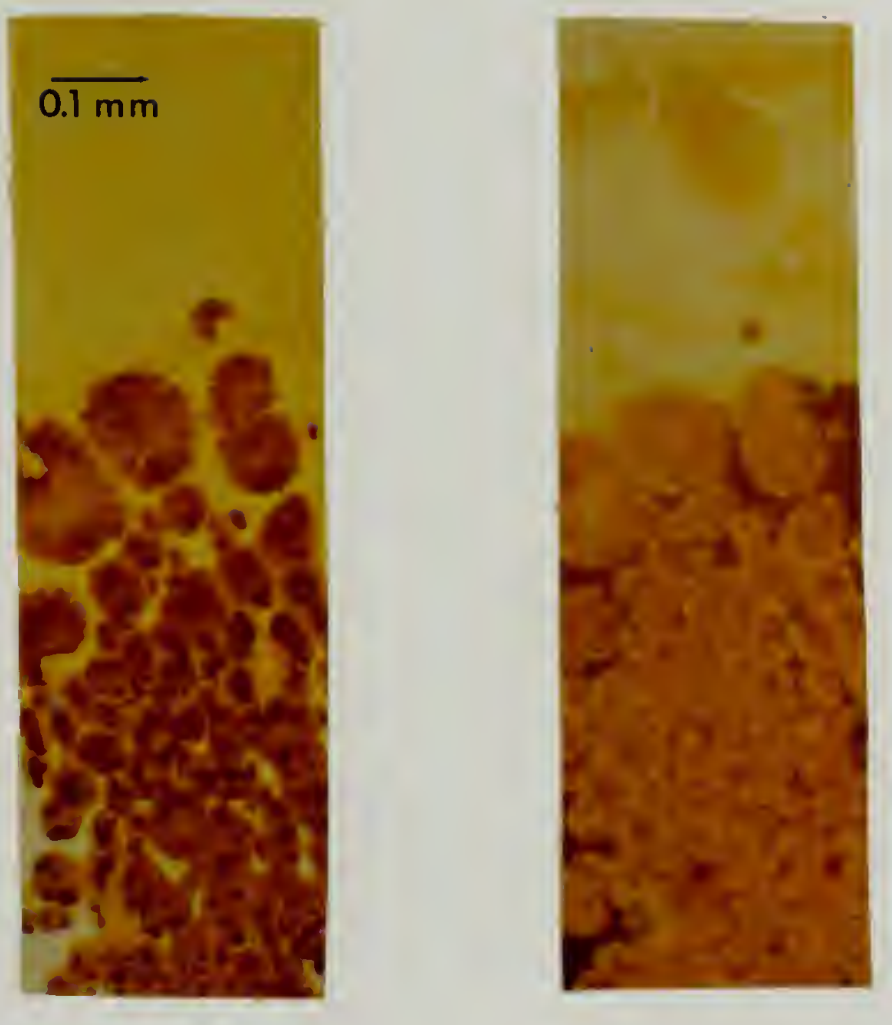

Figure 4.7

Crystal solvates growing from metastable nematic liquid into equilibrium state of crystal solvate plus isotropic liquid.

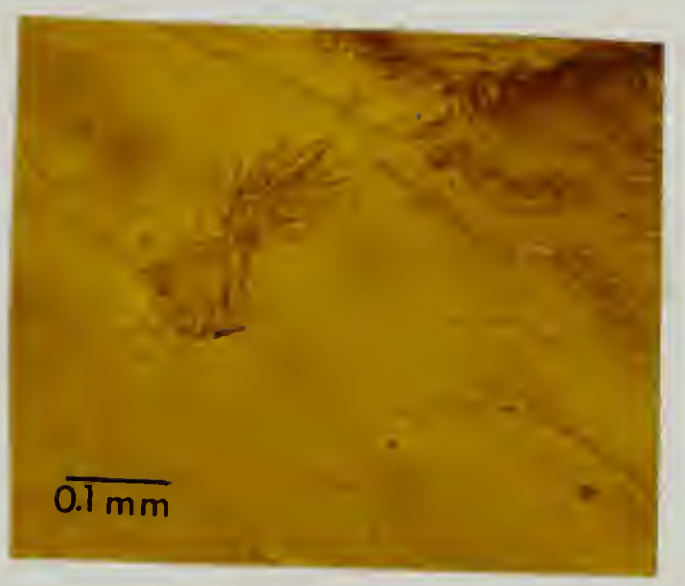

Figure 4.8

A crystal solvate spherulite growing from a nematic solution.

refraction is greater than the radial, indicating tangential orientation of the rod-like PBT molecules. Direct electron microscopy of the crystal solvates was not possible due to the highly corrosive nature of the solvent and the high vacuum of the electron microscope. Instead the MSA was first leached out by floating the spherulites off the glass slide onto water. After the acid was removed, the sample was picked up with grids and viewed in the electron microscope. The tangential orientation of the chains was confirmed by electron diffraction of an area of radiating lamellae as shown in Figure 4.9.

The crystalline nature of the lamella of the residual PBT is shown in the bright field pair shown in Figure 4.10. The lamellar thickness measured from the micrographs, is about 450 angstroms, with the long period being about 700 angstroms. This scale corresponds reasonably with the average molecular length determined by Crosby et al. for PBT of I.V. 2.0. The question of what is in the interlamellar region in a polymer that is essentially 100% crystalline is an interesting one. Gardner proposes a model for PPTA fibers which has a high concentration of chain ends in the periodic bands first observed by Dobb et al. [15,16]. In our system the close correspondence of molecular length to the lamellar thickness suggests a similar model. A schematic of this type of morphology is shown in Figure 4.11. Aggregation of chain ends in the interlamellar region

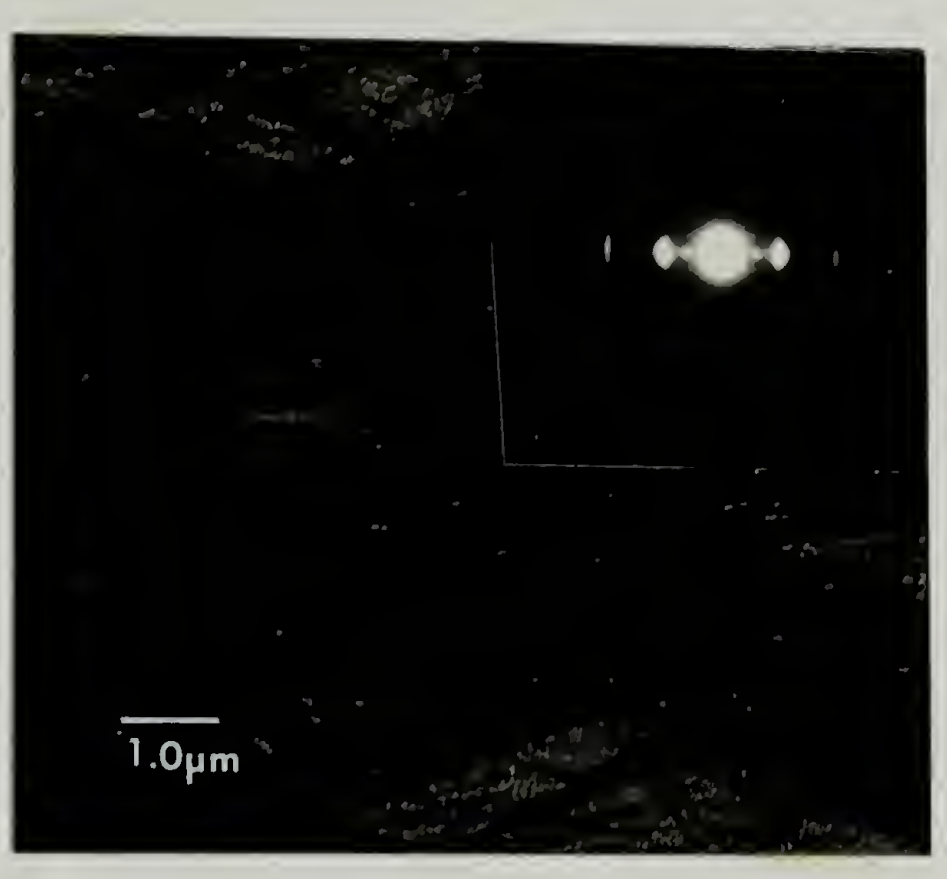

Figure 4.9

PBT lamellae remaining after solvent removal and drying. Electron diffraction (inset) reveals the chain orientation is perpendicular to the lamellae.

Figure 4.10

Bright field/dark field pair (a and b respectively) showing lamellae and fracture paths of lamellar region of PBT.

a.

b.

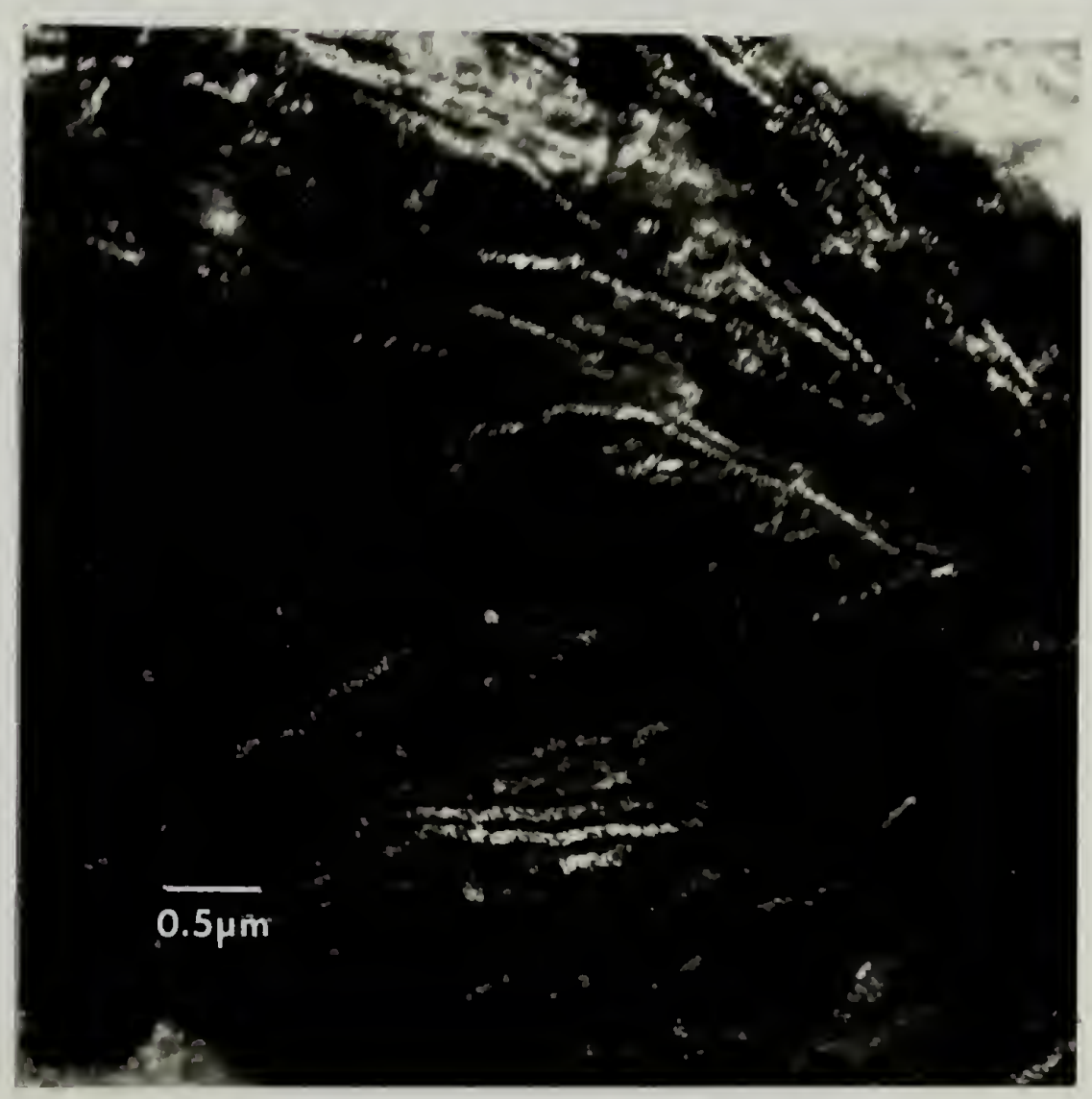

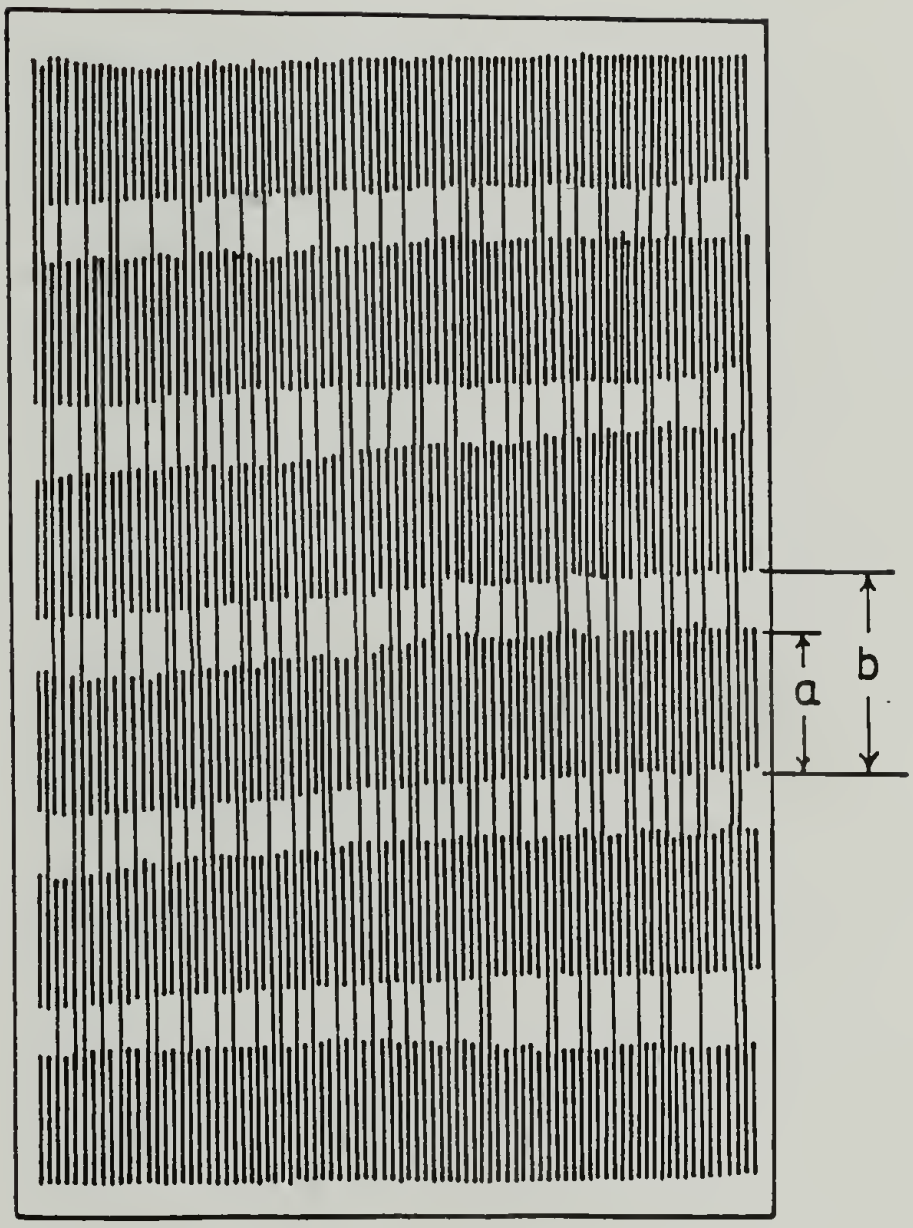

Figure 4.11

Schematic of proposed lamellar structure of PBT. a. corresponds to lamellar width, b. corresponds to long period.

would be favored for low I.V. PBT. According to the synthetic route proposed by Wolfe, et al. [17], it can be seen that there would be poly(phosphoric acid) covalently bonded to the ends of the molecules. Closer examination of these micrographs reveals that the film fracture generally takes place perpendicular to the lamellae, or alternatively, between them. Since the chains run perpendicular to the lamellae, fracture between lamellae is further evidence of a high concentration of chain ends in the interlamellar regions.

The texturing in these lamellae is observable through electron diffraction. For a PBT fiber a typical equatorial intensity profile would appear as in Figure 4.12. The peaks e1 - e4 are as indicated. The presence of all of these reflections in electron or x-ray diffraction with their relative intensities is generally evidence of fiber symmetry.

In these spherulites of PBT, however, a variety of diffraction patterns consisting of e1 - e4, e1 and e2, just e2, and e2 and e3, with their relative intensities, have all been observed. Upon tilting the sample, the pattern is shown to change with e1 appearing and disappearing with various degrees of tilt (e.g.Fig.4.13). This indicates that there is not fiber symmetry, but rather locally preferred $\underset{\sim}{a}$ axis and $\underset{\sim}{b}$ axis orientations. Further evidence for texturing is found in the micrographs of Figure 4.10.

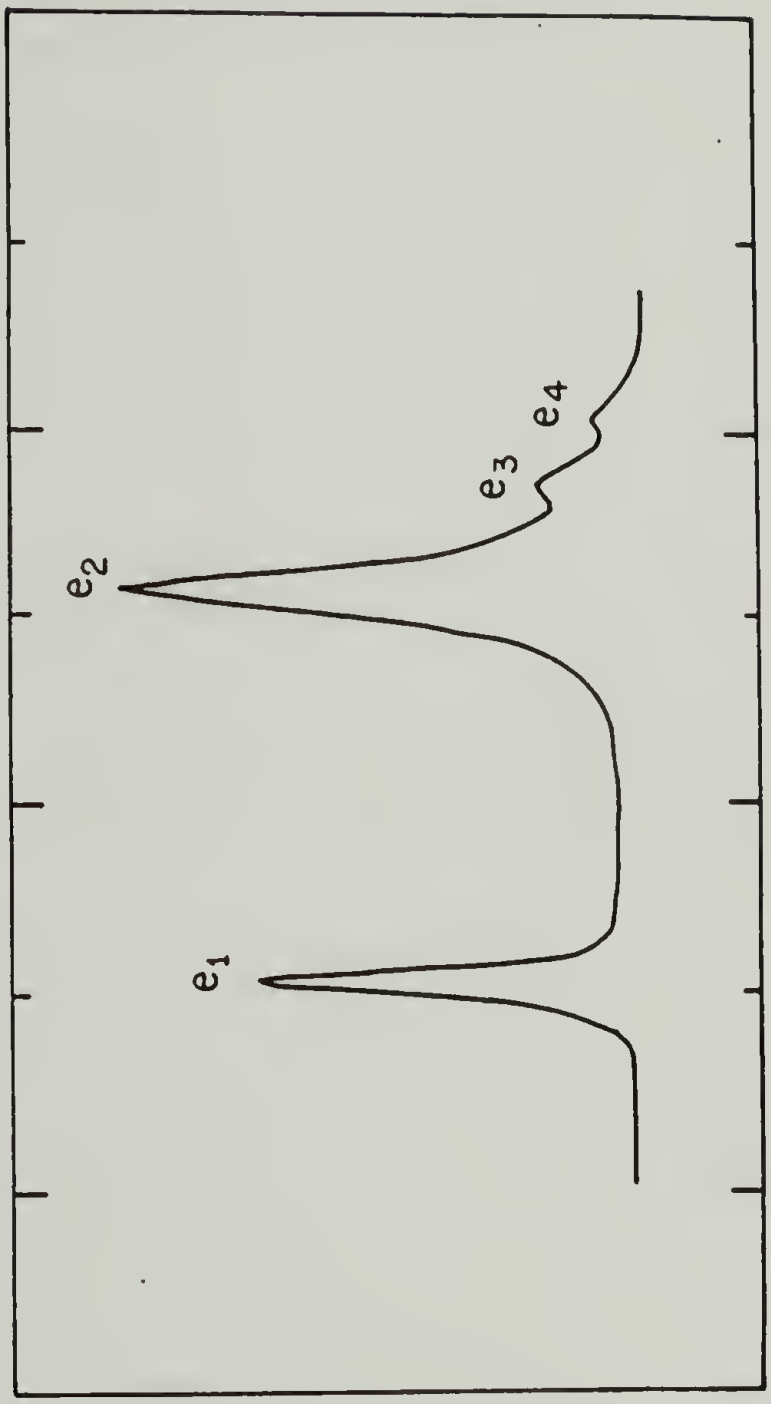

Figure 4.12 Equatorial 2θ scan of PBT fiber [19].

Figure 4.13

Electron diffraction data revealing texturing in PBT. a. e1 - e4 all present in typical fiber symmetric intensities, b. e1 and e2 only, c. e2 only, d. e2 and e3 only with e2 being more intense, e. e2 and e3 only with e3 being more intense.

a.

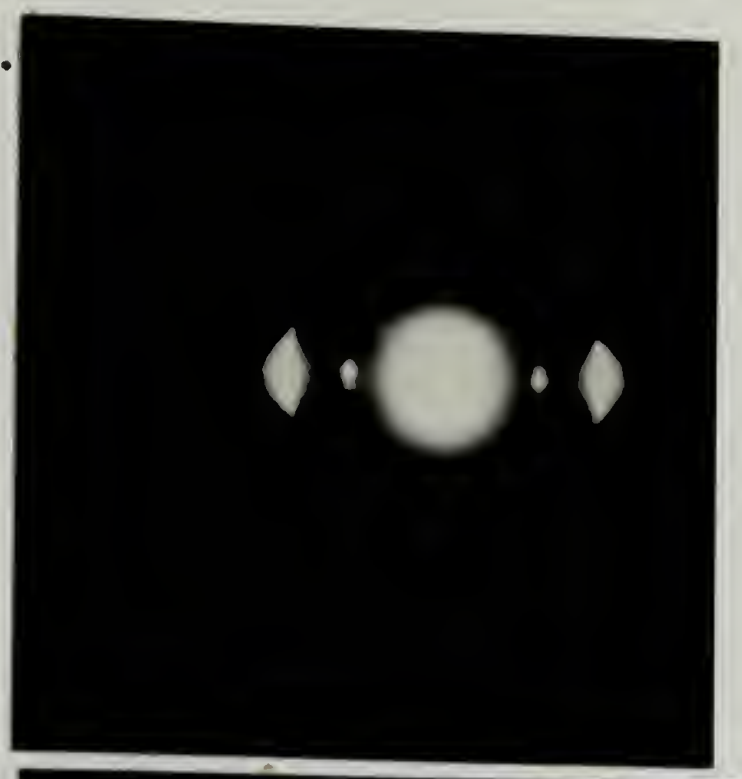

b.

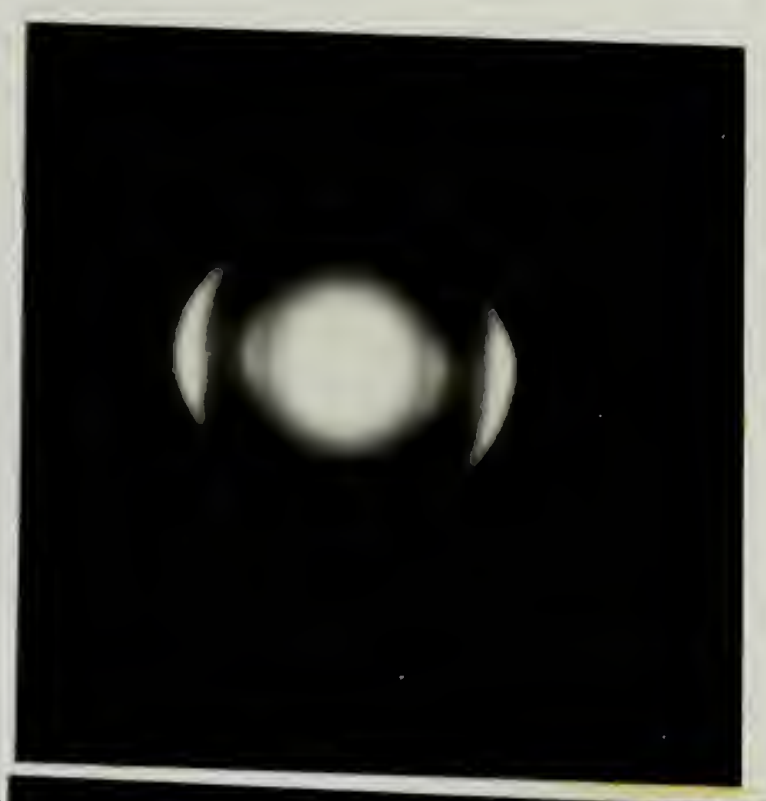

c.

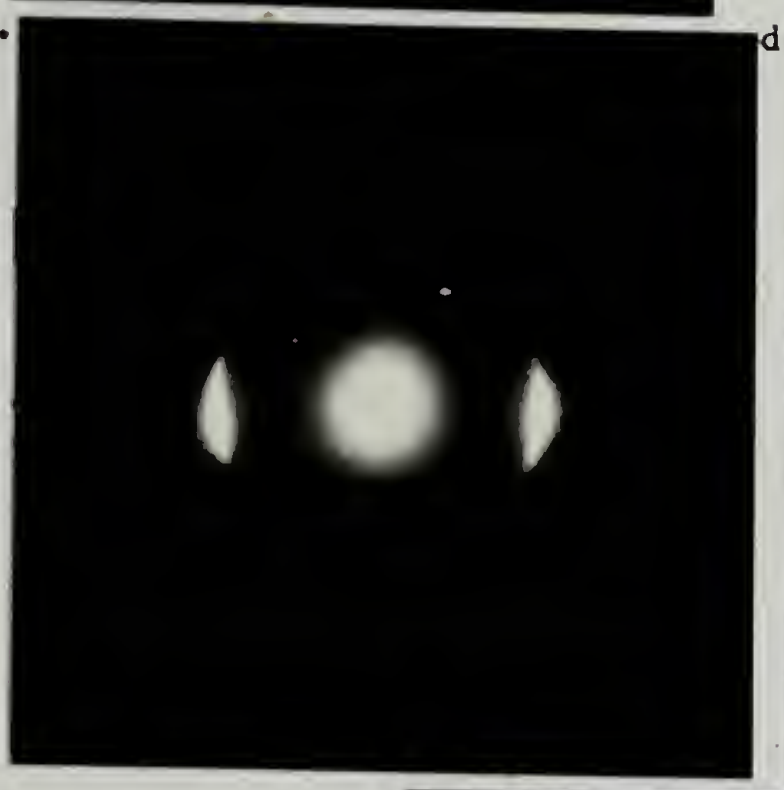

d.

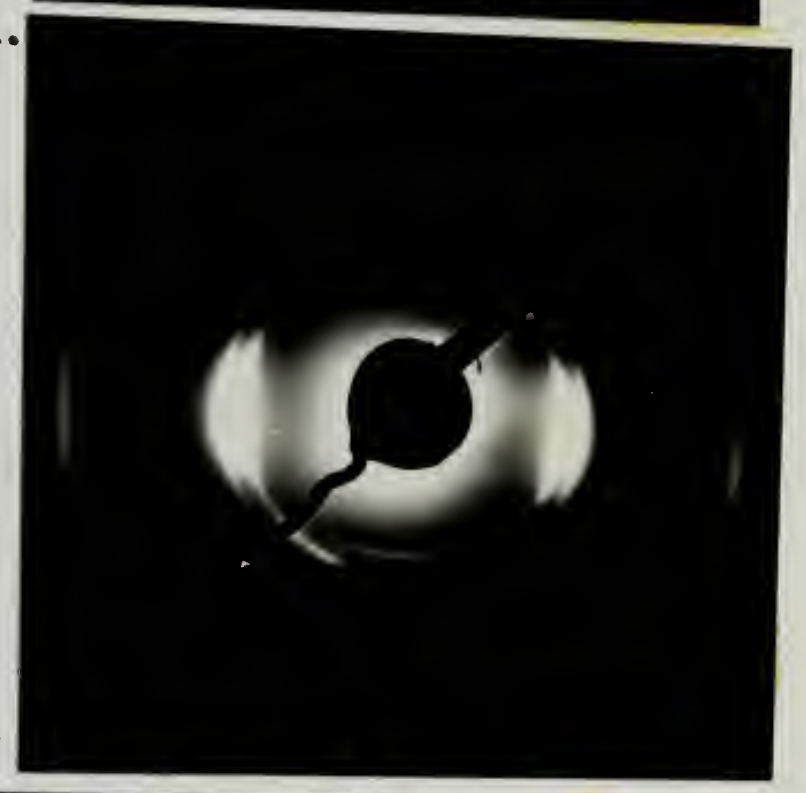

e.

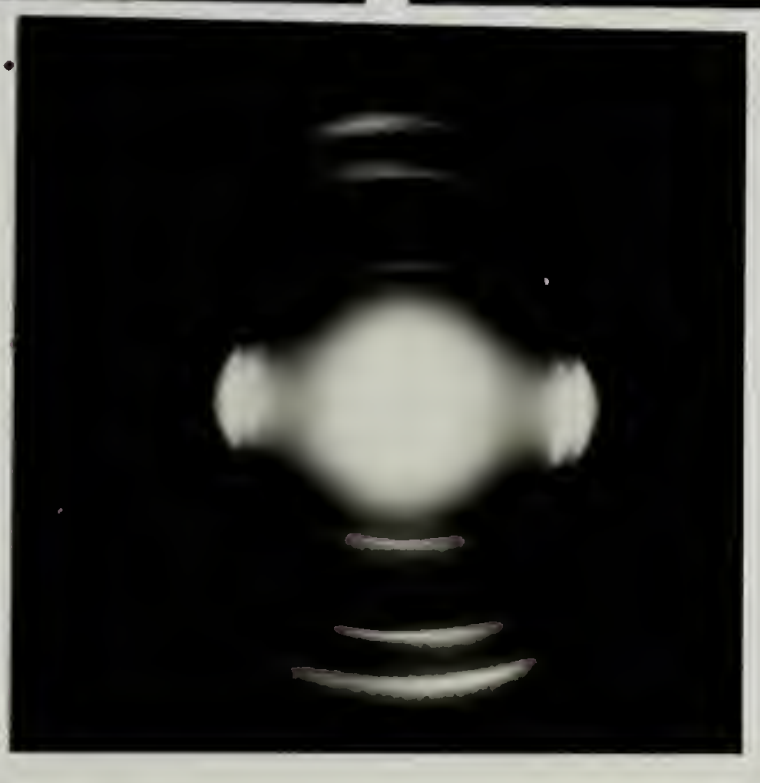

In bright field, the lamellae appear as continuous structures, whereas the dark field micrograph shows individual crystallites about 150 angstroms in width by 450 angstroms in length.

Figure 4.14 shows a lamellar region of a PBT spherulite, very similar in appearance to Takahashi's PPTA lamellae. A fine structure running perpendicular to the lamellae can be seen to run across the tear in the film. For the sake of comparison, Figure 4.15 shows a "grassy mat" prepared by rapid coagulation of an isotropic PBT/MSA solution into water, similar to what Minter reported for PBO [5].

One other feature of the PBT lamellae spherulites is that electron diffraction down the c axis has been observed for the first time (e.g.Fig. 4.16). The angle (gamma) between the e1 and e2 reflection is about 109 degrees which is not consistent with the monoclinic unit cell with gamma equal to 95.2 degrees proposed by Roche [18]. The e3 and e4 reflections are also present, but very weak; e3 at an angle of about 20 degrees from the e2 reflection and e4 being the second order e1 reflection.

Discussion

Conclusive proof for the existence of PBT crystal solvates has been presented. The melting transitions

Figure 4.14

Bright field electron micrographs of lamellar PBT. a. sheaf like structures readily apparent and b. higher magnification of a. Note fine 100 angstrom cross-hatching perpendicular to lamellae.

a.

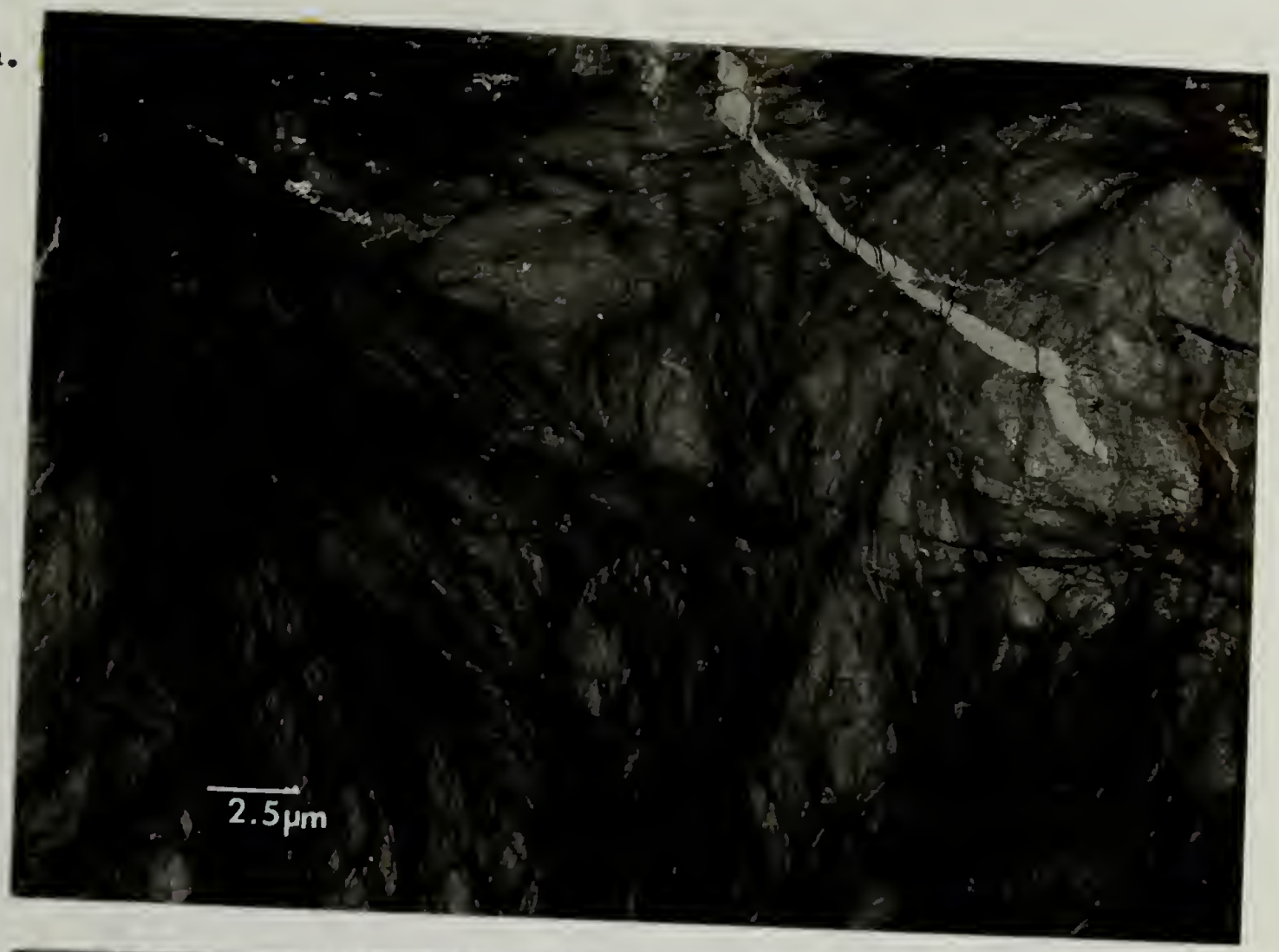

b.

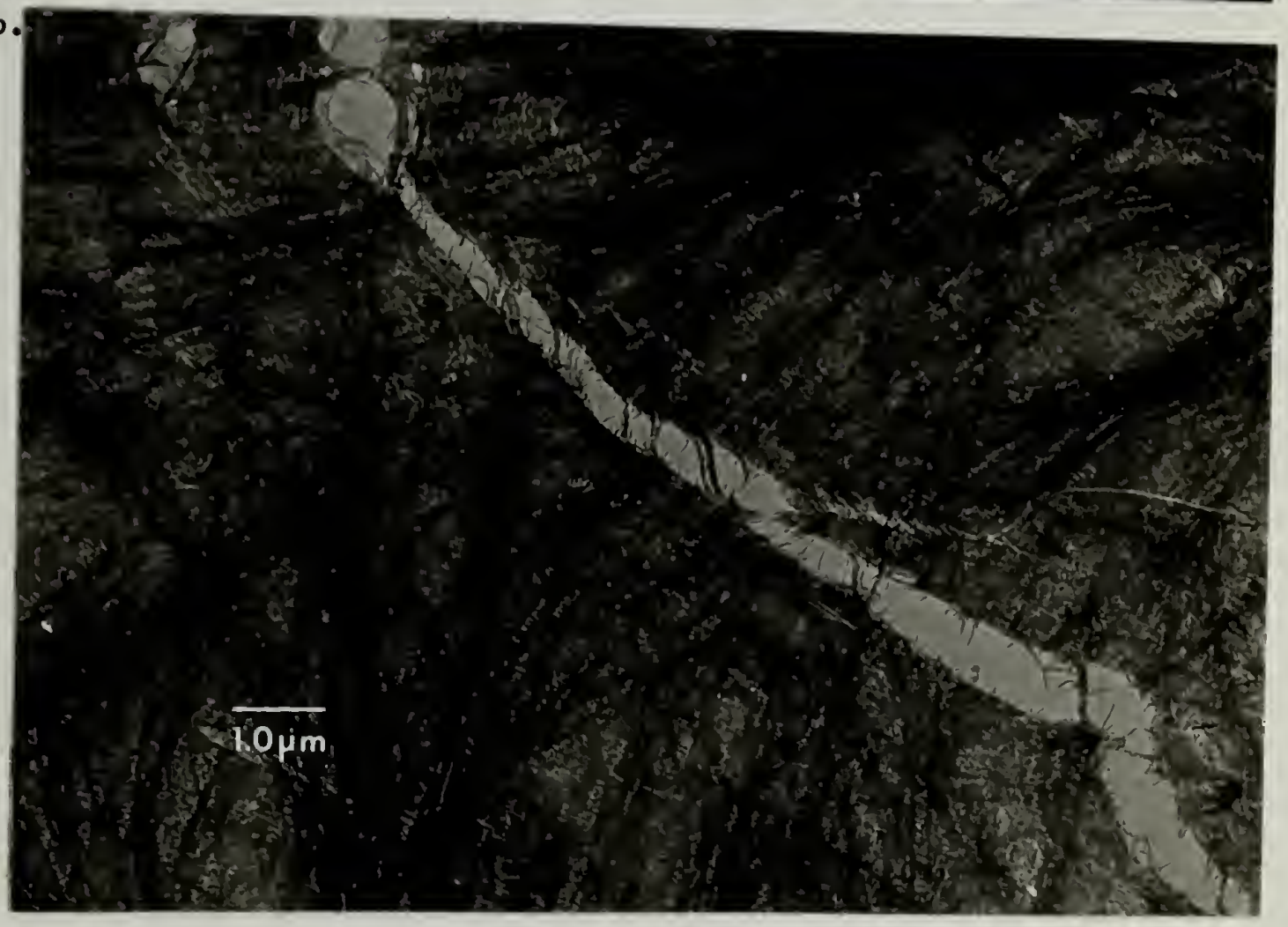

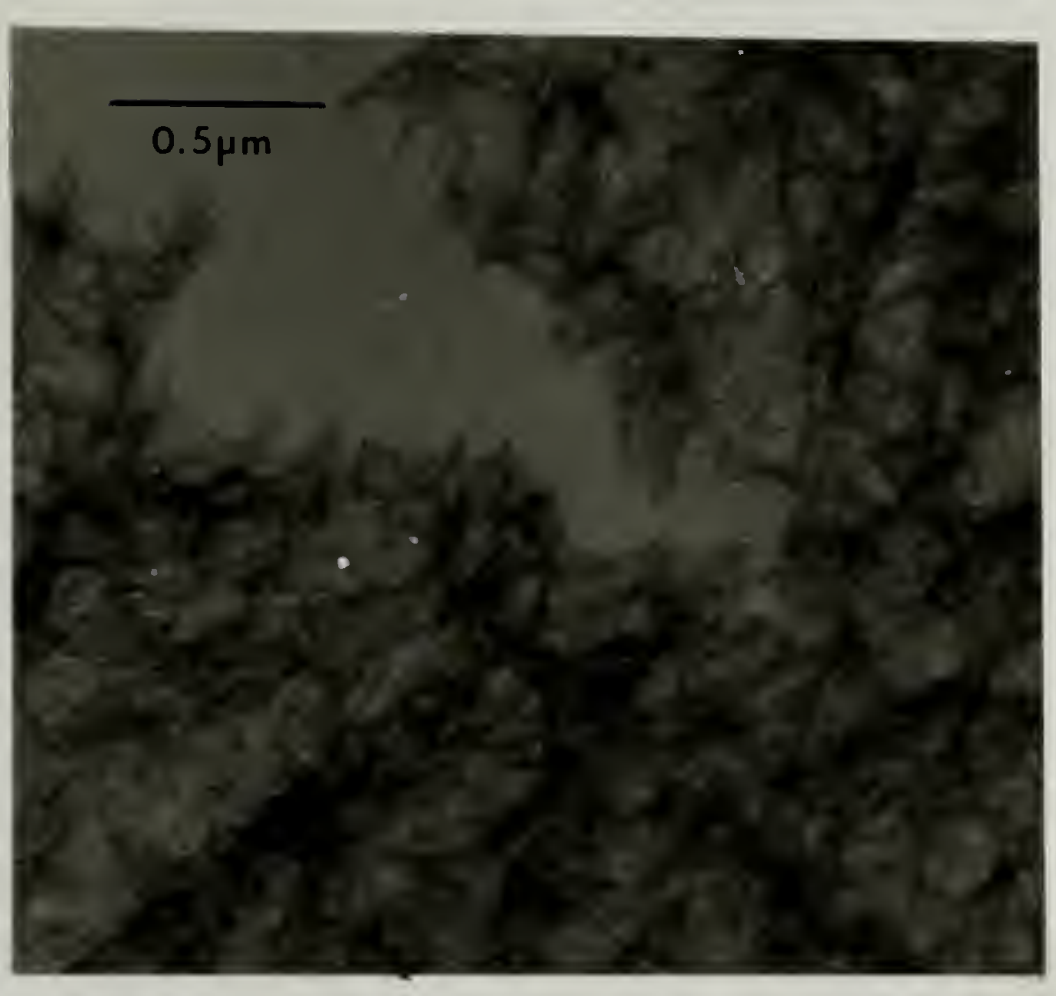

Figure 4.15

Bright field image of "grassy mat" formed by coagulation of isotropic solution.

a.

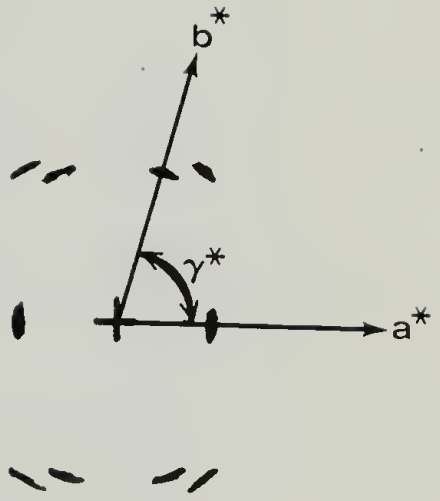

b.

Figure 4.16

a. electron diffraction of the a b plane of a twinned crystal. C axis is perpendicular to the page,
b. schematic of diffraction pattern.

observed by DSC and optical microscopy, coupled with the x-ray diffraction pattern of the anisotropic solid show that a crystalline solid(s) containing both polymer and solvent is (are) formed in this system. The existence of two strong melting transitions and a weaker third transition, all observed both by DSC and optical microscopy give evidence for the existence of at least one and probably two or three crystal solvates.

Upon removal of the solvent the optically negative crystal solvate spherulites remain optically negative. This is indicative of retention of the gross morphology upon transformation from crystal solvate to crystalline polymer. The crystalline polymer is highly ordered as revealed by observation under the electron microscope. It seems reasonable that the existence of lamellae in the crystalline polymer point to the existence of lamellar forms in the crystal solvate spherulites.

Examination of the electron diffraction patterns obtained from the PBT spherulites reveals a highly textured morphology. The existence of the individual crystallites in the dark field micrograph of the continuous lamellae in Figure 4.10 supports this. Specific reasons for why the lamellae are broken by sections in the Bragg condition and out of the Bragg condition are not understood. It is, however, a feature that is not exclusive to PBT, but is also found in polyethylene [20] and PPTA [6]. Whether or not

this is related to the 100 angstrom striations observed in Figure 4.14 is not clear. The sample preparation of the electron microscopy grids involved the placing of the crystal solvate in equilibrium with an isotropic solution into water. Since rapid coagulation of PBT solutions gives rise to a fibrillar mat, these striations may be a result of the coagulation of the remaining isotropic solution. However, they run more or less parallel to each other and are not randomly oriented as they would be in a coagulated film. One thing is clear: the final morphology of PBT is highly path dependent. Very slow diffusion of limited amounts of water leads to lamellar crystal solvate spherulites, which when washed, leave crystalline lamellar PBT spherulites. Very rapid addition of copious amounts of water to PBT solutions yields fibrillar polycrystalline mats of PBT.

The phase behavior of this system is consistent with the schematic given by Iovleva. Because there probably exist at least two crystal solvates, however, the schematic must be modified slightly. The phase boundaries of the chimney region for PBT in MSA were obtained by Tsai [21]. Proper adjustment for the different MW they used shifted the chimney to the right for our study according to the relationship $V2^* = 8/x(1-2/x)$, where x is the aspect ratio and $V2^*$ is the characteristic concentration for the appearance of the chimney region. The observation of

melting at 90 degrees C, together with nematic to isotropic clearing at elevated temperatures indicates the chimney region occurs at higher temperatures than the crystal solvate and therefore nematic solutions can occur at equilibrium. However, the fact that the higher melting crystal solvates melt into isotropic solutions indicates that the chimney region curves and crosses the crystallization curves.

Ciferri and Krigbaum's theoretical work supposes an equilibrium with crystalline polymer. Their treatment is even more applicable to polymeric systems with the inclusion of crystal solvates. Lower melting transition temperatures and heats of fusion would be true of crystal solvates as compared with crystalline polymer. We have shown here that a treatment of the phase behavior by superposition of liquid-liquid and liquid-crystal phase diagrams helps to explain the observations in the PBT/MSA·H_2O system.

Understanding of this type of phase behavior can help to explain some of the experimental observations in the literature. Sasaki et al. have studied the PBLG/BA system [22]. They have observed two gels, A and B, of different stoichiometric polymer/solvent ratios. Experimentally, the B type gel is obtained by repeated quenching from 60 degrees C to below 48 degrees C. This puts the system in an unstable state, with regard to the equilibrium crystal or crystal solvate, but also with respect to the liquid-liquid phase

diagram. Liquid-liquid phase separation is kinetically favorable and gives an anisotropic solution of composition that must be greater in polymer than that of the crystal solvate, not to precisely the crystal solvate composition as claimed. This is unstable with respect to crystalline polymer and crystal solvate, so phase separation to these two solid forms occurs. Heating to 60 degrees C melts the crystal solvate while the crystalline polymer retains its solid form. Quenching again gives the same behavior of liquid-liquid phase separation followed by solid-solid phase separation of the anisotropic solution. Thus B gel grows at the expense of A gel. The observations of Sasaki et al. are more easily interpreted using this type of treatment of phase behavior.

Inclusion of crystal solvates in the Ciferri-Krigbaum phase relationship enables significantly better understanding of the experimental observations in the present PBT work, as well as in other systems such as PBLG/BA.

Conclusions

Growth of crystal solvates in the PBT/MSA system has been accomplished for the first time through the diffusion of water into the system. Identification of the solid as crystal solvate was accomplished by diffraction and thermodynamic measurements. In this way, evidence for the

existence of at least one and possibly two or three crystal solvates has been obtained.

Upon observation under an optical microscope negative spherulites from this system were observed. The tangential orientation of the rigid PBT chains in the spherulites indicated by the optical microscope were confirmed using an electron microscope for both direct visualization and diffraction studies of residual dried PBT.

The crystalline PBT left as a residue upon removal of the acid solvent was also investigated. Lamellae were observed whose thickness corresponds closely with the molecular length of the PBT used. The path dependent morphology of these samples was discussed and texturing of the PBT was described. For the first time a c axis projection electron diffraction pattern is obtained and reported. This represents the first significant departure from the unit cell obtained by Roche et al. and points to the probability of polymorphism for PBT.

Phase behavior after the Ciferri and Krigbaum approach is investigated and a pseudo-binary schematic phase diagram for the PBT/MSA·H_2O system is presented.

C H A P T E R V

FUTURE WORK

The work that has been presented here, coupled with some preliminary observations noted below, suggest several avenues for subsequent investigation.

The unit cell of PBT previously obtained by Roche et al. [18] was obtained by fiber diffraction perpendicular to the chain axis. Calculations from the intensities of the equatorial and layer line reflections were used to obtain the value for gamma of 95.2 degrees [18]. Attempts by Minter to stack films and view the c axis by x-ray diffraction were inconclusive [5]. No electron diffraction data has previously been obtained viewing down the c axis. The low MW of the PBT used in this study, along with the path of crystal formation, allowed this type of diffraction data to be obtained (e.g. Fig.4.16). The difference in sample history is consistent with polymorphism. However, the reflections are not sharp enough to allow determination of gamma closer than plus or minus 5 degrees. It is expected that through further study of crystalline PBT crystallized through the crystal solvate intermediate, better diffraction data can be obtained directly. This data, along with data from tilting about the c axis should give a well-defined unit cell and crystal structure for PBT crystallized in this way.

While generally solvent was washed out of the samples used in electron microscopy, occasionally diffraction patterns were obtained that were clearly not PBT, but rather a crystal solvate of PBT (e.g. Fig.5.1). Further work along these lines would enable the crystal structure of the crystal solvate to be determined, provided the stoichiometric ratio of PBT to MSA was also ascertained. Since more than one PBT/MSA crystal solvate is believed to exist, it would be useful to ascertain the crystal structure of each type.

Characterization of the polymorphs of the crystal solvate would be helpful in knowing if, after washing, the residual PBT also exhibits polymorphism. Growth of PBT/MSA crystal solvates includes growth from isotropic, anistropic and biphasic regions (e.g. Fig.5.2). The path dependency of the morphology could be investigated by examining the crystal solvates grown from each phase.

It was also observed by optical microscopy that PBT dissolved in PPA and very slowly precipitated in ortho phosphoric acid produced an orange solid that melted at 70 degrees C into an isotropic solution. Upon standing it was observed to crystallize from the outside of the cover slip in with the passage of time and corresponding diffusion of water.

An unexplained observation of the PBT/PPA system was also made. When this orange solid was placed on a glass

a.

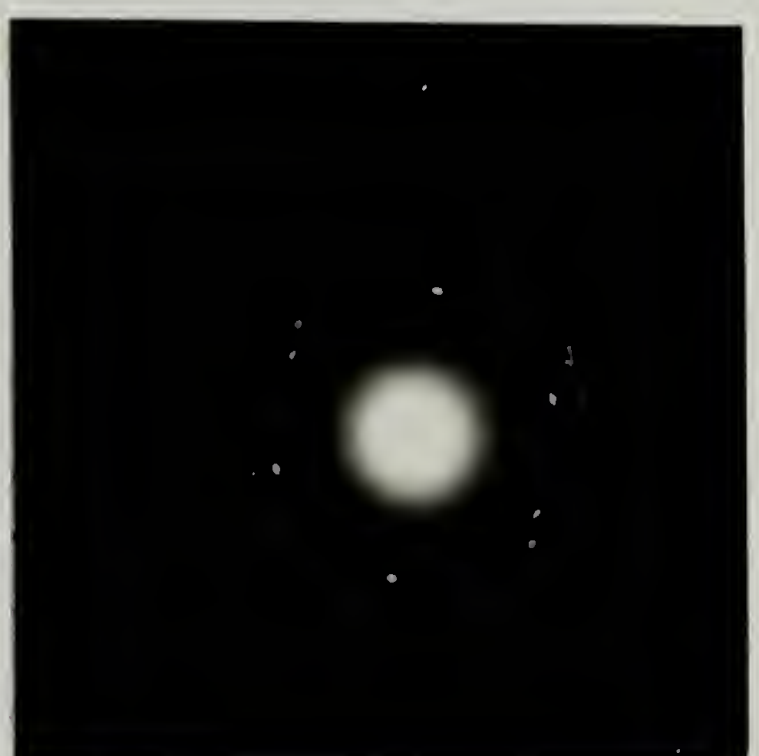

b.

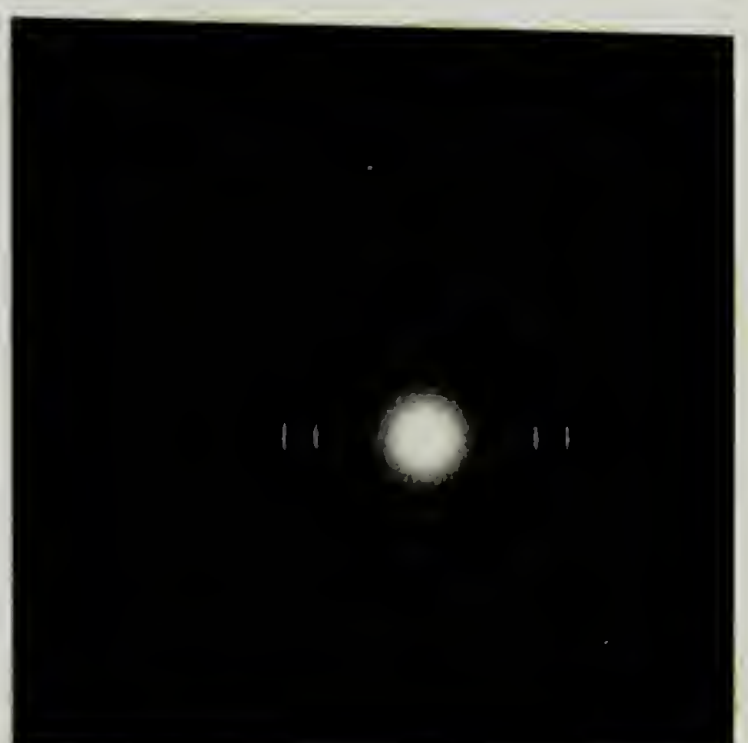

Figure 5.1

Examples of crystal solvate diffraction. Pattern a has the e2 PBT arc superimposed upon it.

a.

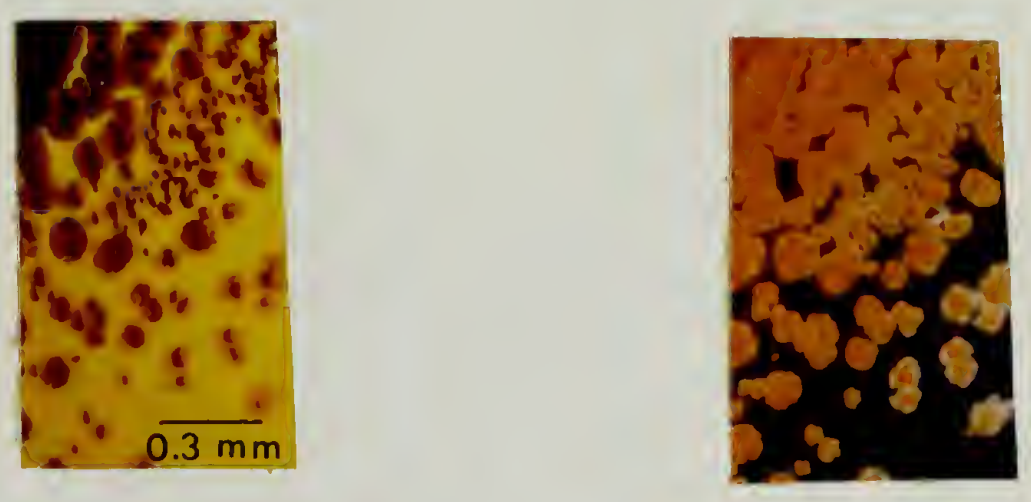

b.

c.

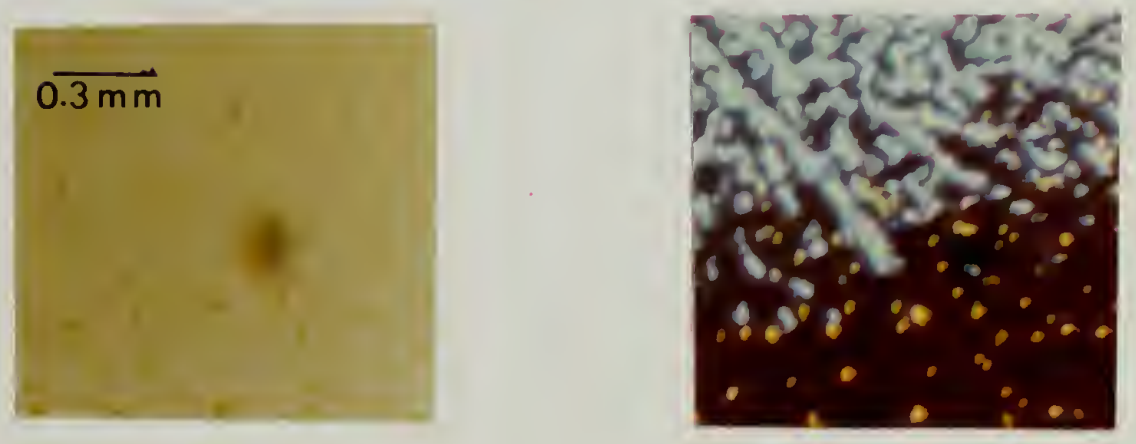

Figure 5.2

Crystal solvate growth from a. isotropic, b. anisotropic and c. biphasic solutions. Left: analyzer removed, Right: polarizer and analyzer crossed.

slide, covered with a cover slip, and then placed onto a preheated (200 degrees C) hot stage of an optical microscope, melting to an isotropic solution followed by rapid nucleation and growth of spherulites was observed. Whether this is due to a change in the solvent, PPA, or to some more complicated phase change is not known.

One further extension of this work would be to investigate poly(p-phenylene benzobisoxazole) (PBO) to see if it also gives rise to crystal solvates. The unit cell of PBO has not yet been determined and crystallization of low MW PBO through the crystal solvate intermediate may provide a straightforward means of determining it. It now seems that PBO may be at least as useful as PBT as a high-modulus high-strength material and investigations of PBO could prove to be singularly important.

REFERENCES

1. H.Sobue, H.Kiessig, and K.Hess, Z. Physik. Chem., B43, 309 (1939).
2. M.M.Iovleva and S.P.Papkov, Vysokomol. soyed., A24, 233 (1982). (translated in Polym. Sci. USSR., 24, 236 (1982).
3. M.M.Iovleva, V.N.Smirnova, Z.S.Khanin, A.V.Volokhine, and S.P.Papkov, Polym. Sci. USSR., 23, 2048 (1981).
4. C.R.Crosby,III, N.C.Ford,Jr., F.E.Karasz, and K.H. Langley, J. Chem. Phys., 75, 4298 (1981).
5. J.Minter, Ph.D. Thesis, University of Massachusetts, 1982.
6. T.Takahashi, H.Iwamoto, K.Inove, and I.Tsuji-oto, J. Polym. Sci., Polym. Phys. Ed., 17, 115 (1979).
7. V.A.Platonov, Diss, Cand, Chem. Sci., NPO, Khimvolokno, Mytischi (1978).
8. M.M.Iovleva, S.I.Bandviyan, N.I.Ivanova, V.A.Platonov, L.P.Mil'Kova, Z.S.Khonim, A.V.Volokhina, and S.P.Papkov, Vysolomol. soyed., B21, 351 (1979).
9. L.Onsager, Ann. N.Y. Acad. Sci., 51, 627 (1949).
10. A.Isihara, J. Chem. Phys., 19, 1142 (1951).
11. P.J.Flory, Proc. Royal Soc. London, Ser. A. 234, 73 (1956).

12. A.Ciferri and W.R.Krigbaum, Mol. Cryst. Liq. Cryst., 69, 273 (1981).

13. K.H.Gardner, R.R.Matheson, P.Avakian, Y.T.Chin, T.D. Gierke, and H.H.Yang, J. Polym. Sci., Polym. Phys. Ed., 21, 1955 (1983).

14. S.Russo and W.G.Miller, Macromolecules, 17, 1324 (1984).

15. M.Panar, P.Avakian, R.C.Blume, K.H.Gardner, T.D.Gierke and H.H.Yang, in press.

16. M.G.Dobb, D.J. Johnson, and B.P.Saville, J. Polym. Sci., Polym. Phys. Ed., 15, 2201 (1977).

17. J.F.Wolfe, B.H.Loo and F.E.Arnold, Macromolecules, 14, 915 (1981).

18. E.J.Roche, T.Takahashi and E.L.Thomas, ACS Symposium Series, 141, 303 (1981).

19. S.Allen, Ph.D. Thesis, University of Massachusetts, 1983.

20. E.L.Thomas, unpublished data.

21. H.Tsai, Ph.D. Thesis, Carnegie Mellon University, 1983.

22. S.Sasaki, K.Tokuma and I.Uematsu, Polymer Bulletin, 10, 539 (1983).